View metadata, citation and similar papers at core.ac.uk
brought to you by CORE
provided by UPCommons. Portal del coneixement obert de la UPC

Electroactive and bioactive films of random copolymers containing terthiophene, carboxyl and Schiff base functionalities in the main chain

Maria M. Pérez-Madrigal,[1,2] Luminita Cianga,[3] Luis J. del Valle,[1] Ioan Cianga,[3,*] and Carlos Alemán[1,2,*]

[1] *Departament d'Enginyeria Química, ETSEIB, Universitat Politècnica de Catalunya, Avda. Diagonal 647, Barcelona E-08028, Spain*

[2] *Center for Research in Nano-Engineering, Universitat Politècnica de Catalunya, Campus Sud, Edifici C', C/Pasqual i Vila s/n, Barcelona E-08028, Spain*

[1] *"Petru Poni" Institute of Macromolecular Chemistry, 41A, Grigore –Ghica Voda Alley, 700487, Iasi, Romania*

[*] Corresponding authors: Ioan Cianga (ioanc@icmpp.ro) and Carlos Alemán (carlos.aleman@upc.edu)

ABSTRACT

A new bis-thienyl type monomer with preformed azomethine linkages (AzbT) was chemically synthesized and, subsequently, electro-copolymerized with 2,2′:5′,2″-terthiophene (Th_3). AzbT:Th_3 mixtures with different molar ratios (*i.e.* 50:50, 60:40 and 80:20) were considered, the resulting thin films being made of random insoluble copolymers, P(AzbT-*co*-Th_3)s. The content of AzbT in P(AzbT-*co*-Th_3)s was found to increase with the AzbT:Th_3 molar ratio in the electropolymerization medium. Furthermore, characterization of the different copolymers suggests the existence of several concomitant processes in the reaction medium. Thus, depending on the composition of the reaction medium, AzbT worked as a co-monomer and/or as a dopant for the growing polymer chains. The morphology of the films evolved from a porous multi-level surface to a more compact and flat globular structure with increasing AzbT content. On the other hand, the electrochemical and optical properties were also influenced by the AzbT:Th_3 ratio. Cytotoxicity and cell adhesion and proliferation tests, which were performed using human osteosarcoma and monkey kidney epithelial cell lines (MG-63 and Vero, respectively), revealed that P(AzbT-*co*-Th_3) matrices can be potentially applied as bioactive substrates. This behaviour was especially relevant for the 80:20 copolymer, which exhibits optical and electrochemical properties in the range of polythiophene derivatives, suggesting that it is a promising functional biomaterial.

INTRODUCTION

Compounds that contain the –C=N– functional linkage in their structure, which are known as Schiff bases (imine or azomethine), are usually synthesized by the condensation of primary amines with compounds bearing active carbonyl groups (*e.g.* an aldehyde). Schiff bases have been applied in a great number of different fields including reactants for organic synthesis,[1,2] inhibition of corrosion[3] and, especially, biological chemistry. Thus, the azomethine functional group exhibits antibacterial and antifungal,[4,5] pesticidal,[6] antitubercular,[7,8] analgesic,[9] antioxidant,[10] anti-inflammatory,[9,10] antidyslipidemic,[11,12] antiviral,[13] antiglycation,[14] and antitumor[15] activities.

In the field of polymers, poly(Schiff base)s or polyazomethines are considered very important materials as long as all the above mentioned properties for Schiff bases are preserved in the polymer counterpart.[16] Furthermore, the presence of –C=N– conjugated double bonds in the main polymeric chain represents a highly attractive alternative to vinylene linkages to display semiconducting properties.[17,18] Thus, polyazomethine-based materials have been exploited for the fabrication of solar cells,[19] fluorescent sensors for explosive or environmentally toxic metal ions,[20,21] electrochromic devices,[22,23] organic field-effect transistors (OFET)s,[24] and organic non-volatile memories (ONVM)s for the next generation of data storage devices.[25]

Another important aspect concerning the azomethine bond is related to its reversibility, a property which was efficiently exploited in the J. M. Lehn's concept of molecular dynamers.[26-28] In that context, dynamic covalent chemistry is a powerful concept for the construction of adaptive and responsive molecular systems. Conjugated

polyazomethines can undergo constitutional exchange resulting in materials with tuneable properties induced by external stimuli.[29,30]

Aromatic polyazomethines can be obtained by different chemical procedures: classical polycondensation between aromatic/ heterocyclic dialdehydes with aromatic/heterocyclic diamines;[18-20,23-25] self-polycondensation of an automer;[32] and polymerization of monomers containing preformed azomethine linkages.[22,29-36] Among these synthetic approaches, the one employing monomers that contain preformed azomethine bonds seems to be more versatile, provided that it permits the introduction in the conjugated main chain of different moieties (*e.g.* thienyl, pyrolyl, naphtyl and aryl) or well-defined polymeric side chains in a controlled manner, thus allowing for a fine tuning of the electrical and/or optical properties of the final materials.

In recent years, we have used different strategies to enhance the behaviour of polythiophenes (PThs) as bioactive cellular matrices for tissue engineering applications. For example, soluble PTh derivatives have been combined with biodegradable and biocompatible insulating polymers to fabricate 2D[37-41] and 3D[42-44] scaffolds; hydrophilic and biocompatible poly(ethylene glycol) (PEG) chains have been grafted to PTh chains to fabricate amphiphilic PTh bottle-brush copolymers;[45-47] and biomolecules, such as small peptides[48] or proteins,[49-51] have been immobilized into PTh matrices using *in situ* polymerization approaches. In this work, we combine our interest in Schiff bases with our expertise on bioactive PThs to investigate a new approach oriented towards the development of new platforms for tissue engineering applications.

The main aim of this work is to fabricate a new functional synthetic biomaterial with optical properties similar to those displayed by semiconducting PThs. For this purpose,

an azomethine-containig bis-thienyl (AzbT) monomer has been chemically synthesized and electrochemically copolymerized with 2,2':5',2''-therthiophene (Th_3). After investigation of the chemical and physical properties of the resulting P(AzbT-*co*-Th_3) copolymers, which were obtained using different AzbT:Th_3 molar ratios, their behaviour as cellular matrices for tissue engineering applications has been also examined. The advantages and drawbacks provoked with the incorporation of the Schiff base functionality incorporation have been determined by comparing systematically the properties of P(AzbT-*co*-Th_3) with those of polyterthiophene (PTh_3). Complete description of the synthetic procedures and measurements, both are provided in the Electronic Supporting Information (ESI).

RESULTS AND DISCUSSION

Synthesis and characterization of the azomethine-containig bis-thienyl (AzbT) monomer

In the literature, both 2-thiophene carboxaldehyde and 3,5-diaminobenzoic acid have been used to synthesize different Schiff bases in conjunction with naturally occurring aminoacids,[52] 2-aminobenzoic acid,[53] or several aromatic monoaldehydes.[54-56] These compounds show interesting properties like antibacterial,[53,54] or anticancer activity,[55] and can also act as useful regents for poisonous metal ions depollution.[56] Moreover, due to the presence of three functional groups in its structure, 3,5-diaminobenzoic acid has been employed in the synthesis of polyamides,[57] polyimides[58] and polyazometines[59] with carboxylic pendant groups. Therefore, inspired by these previous results, we combined

2-thiophene carboxaldehyde and 3,5-diaminobenzoic into a new structure (Scheme 1) that, to the best of our knowledge, has not been reported to date.

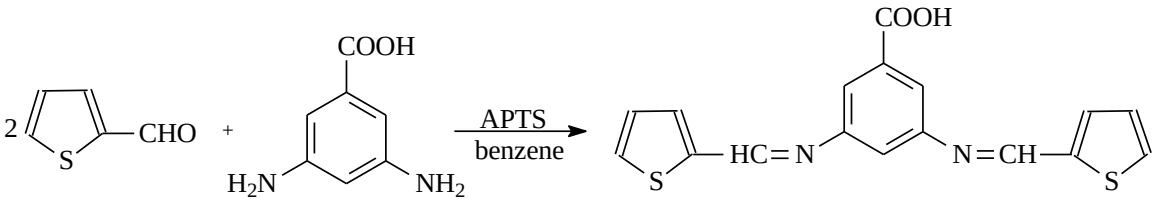

Scheme 1. Synthetic path followed to obtain the AzbT monomer

FTIR and ^{1}H-NMR spectroscopy were complementarily used to confirm the chemical structure of the new-formed AzbT monomer. Complete description of the absorption peaks and resonances is provided in the ESI. Figure S1, which compares the FTIR spectrum of the synthesized monomer with that of 3,5-diaminobenzoic acid, confirms the presence of the thienyl rings in the AzbT monomer. Moreover, absorption peaks attributed to the vibration of NH_2 functional groups, which are present in the IR spectrum of starting 3,5-diaminobenzoic acid, disappear in the spectrum of the AzbT monomer. A shallow peak centred at 1910 cm^{-1} appeared in the spectrum of AzbT that could be attributable to the 1, 3, 5-trisubstituted benezene ring.[60] The presence of the thiophene (Th) rings as well as of the trisubstituted benzene ring in the synthesized monomer was also confirmed by the multiplet in the interval comprised between 6.8 and 7.8 ppm of the ^{1}H-NMR spectrum (Figure 1a). The two singlets at 8.75 ppm and at 8.9 ppm have been assigned to the *syn*- and *anti*-isomers of the azomethine group.[61,62]

^{13}C-NMR and HMQC spectra were recorded in DMSO-d_6 due to AzbT solubility reason. Because this solvent contains water, the ionization of the carboxylic group in AzbT monomer cannot be avoided the more as the preparation of the solution and the

scanning time was long enough so that this process is taking place. Consequently, due to the presence of the acidic protons in the medium, the azomethine linkage can be ripped and reformed in a dynamic manner. The assignment of all the signals in the 1D NMR spectrum (Figure 1b) was performed using the 2D HMQC spectrum (Figure S2). In the spectrum in Figure 1b colored bullets were used with the same color as those of the compounds molecular formulas for pointing out the peaks provenance of each type as they are fixed in the molecular formula of AzbT (black). It also must be stressed that in the non-symmetrical compound in Figure 1b, (red formula), each carbon atom is not equivalent with each other but the position of them not differ very much in comparison with AzbT, fact that could be explained by the presence of the small peaks also discernible in the spectrum.

UV-vis absorption and fluorescence emission (λ_{ex} = 298 nm) spectra of the new monomer dissolved in DMSO are presented in Figure S3. The UV-vis spectrum shows one sharp absorption maximum centered at 289 nm and a shallow one centered at 340 nm. The first peak has been assigned to the π-π^* transition in the tri-substituted benzene ring, while the second one has been attributed to the π-π^* transition of the conjugated sequence formed between the thienyl moieties and the benzene ring, which are connected by the –C=N–bond. On the other hand, AzbT emits in both violet and blue regions with peaks at 360 nm and 490 nm, respectively.

Synthesis of random copolymers P(AzbT-co-Th$_3$)s and of PTh$_3$

P(AzbT-*co*-Th$_3$)s and PTh$_3$ films were prepared by chronoamperometry (CA) using acetonitrile and tetrabutylammonium tetrafluoroborate (TBATFB) as solvent and dopant

agent, respectively. Complete description of the polymerization procedure is provided in the ESI. Even though a number of different experimental conditions were tested for the electropolymerization of AzbT alone (*i.e.* varying the solvent, electrolyte, electrode and/or potential), no polymer was obtained. For this behaviour of AzbT in the given conditions several explanations could be possible. The first one is related to the presence of carboxyl as electron-withdrawing group and to the conjugated short chain-like structure, which could hinder electrochemical polymerization by a high oxidation potential. Thus, radicals derived from monomers of high oxidation potentials undergo rapid reactions with the solvent or anions to form soluble products rather than to electropolymerize.[63] Moreover, the anodic polymerization of thiophenes with reactive functional groups (*e.g.* -NH_2, -OH and –COOH) has been reported to be difficult due to their substantial nucleophilicity.[64] On the other hand, in acetonitrile–TBATFB mixture, during the electropolymerization process, a protonation of this medium could take place most probably by ionic dissociation of the carboxyl group.[65] Into an organic medium of a higher acidity, the azomethine linkages can undergo a dynamical exchange that possibly could compete with the polymerization reaction.[29] More details are provided in the ESI.

In order to overcome this limitation, Th_3 was added to the polymerization medium, the presence of which allowed the incorporation of AzbT structural units in the main chain of the copolymers, a strategy already known as a successful one for the obtainment of polymeric material with functional, reactive groups.[64] Cyclic voltammograms recorded for anodic oxidation of Th_3 solution and for solutions of mixture AzbT:Th_3(molar ratios 50:50 and 80:20) in acetonitrile, in the presence of 0.1 M TBATFB, are shown in Figure 2.

Five anodic processes with anodic peak potentials at 1.01 (O_1), 1.14 (O_2), 1.31 (O_3), 1.70 (O_4) and 1.82 V (O_5) are detected in the voltammogram of the Th_3 solution, whereas two anodic processes appear at 1.15 / 1.40 (O_1) and 1.76 / 1.82 V (O_2) in the voltammograms of the 50:50 / 80:20 AzbT:Th_3 solutions. The cyclic voltammogram obtained from the 60:40 AzbT:Th_3 solution, which is displayed in the ESI (Figure S4), was practically identical to that of the 50:50 mixture. According to these results, potential of 1.00 V was considered for the anodic generation of PTh_3 film. Polymerization potential for film generation of P(AzbT-*co*-Th_3)s was established as 1.05 V when AzbT:Th_3 molar ratios were 50:50 and 60:40, while 1.15V was appropriate for film generation at 80:20 molar ratio. These polymerization potentials, which are very close to the oxidation potential O_1 discussed above (Figure 2), allowed us to (1) maximize the velocity of polymerization process and (2) avoid the undesirable overoxidation of the electrogenerated materials, which were deposited onto ITO electrodes.

The polymerization time used to prepare the PTh_3 and the three P(AzbT-*co*-Th_3) copolymer films was set at θ = 150 and 180 s, respectively. These values for the polymerization time were found to be the most appropriate to obtain high quality films without compromising the optical properties of the resulting systems. Detailed discussion of the variation of the optical properties with the polymerization time is provided in the ESI (Figure S5).

XPS spectroscopy

The films surface composition of P(AzbT-*co*-Th_3) copolymers was evaluated by XPS spectroscopy in an attempt to assess the proportion of the AzbT structural units in the

copolymers. Spectra in the B1s and F1s regions (not shown) for PTh_3 and the three compositions of P(AzbT-*co*-Th_3) films show a sharp peak at 193.8-194.3 and 685.8-686.2 eV, respectively, which correspond to the B–F bonds of the dopant agent.[63,64] Table 1 summarizes the atomic percent composition of PTh_3 and the three copolymers as resulted by XPS. The B/S ratios obtained using such atomic percent compositions were directly associated to the doping level (DL in Table 2), which corresponds to the number of positive charges per thiophene ring. The doping level is relatively high for PTh_3, DL= 0.71, indicating that the formula of the oxidized polymer produced by CA is: $\{(Th^{0.71+})_3]_n (BF_4^-)_{0.71 \cdot 3n}\}_{solid}$. However, the doping level decreases drastically upon the incorporation of AzbT in the polymerization medium, as it is revealed by the very low value of DL (0.19) obtained for the 50:50 copolymer. This effect is accompanied by a reduction in the charge consumed during the polymerization process (Q_{pol} in Table 2). Thus, the value of Q_{pol} determined for PTh_3 (Table 2), which was directly obtained from the chronoamperogram recorded during the polymerization process, decreases by ~25% for 50:50 AzbT:Th_3 composition. Results obtained for the copolymer prepared using 60:40 AzbT:Th_3 composition were fully coherent with the previous observations, as it is reflected in Table 2.

These phenomena could take place based on the following two possible scenarios. First, AzbT hiders the electropolymerization of Th_3 promoting the formation of a closed cross-linked structure in which the presence of long linear Th-chains seems to be unfavorable. Second, the ionized form of the AzbT (*i.e.* AzbT-COO^-) present in the medium could work as a doping agent in competition with BF_4^-. Also, while BF_4^- doping is a conventional diffusion-controlled slow process, "*rapid doping*" could be achieved by

the release of protons from the ionizable carboxyl function of AzbT, resulting in so-called "*self- or autodoping polymers*".[64] All of these trends could have as a result the experimentally observed decreased value of DL in relation with BF_4^-. Details about these processes are discussed in the ESI.

The above described situation is changing when the AzbT:Th_3 is increased. Thus, the doping level in relation with BF_4^- increases noticeable for 80:20 copolymer (DL=0.59). Consistently, the Q_{pol} is only ~9% lower than that of PTh_3 (Table 2). These features suggest that, although AzbT seems to preclude the incorporation of Th_3 monomers, the molar ratio of the latter in the polymerization medium is low enough to reduce significantly the formation of cross-links with respect to 50:50 P(AzbT-*co*-Th_3). This results in an opened structure that facilitates the incorporation of dopant anions and the oxidation of polyaromatic fragments.

On the other hand, if the existence and presence of AzbT-COO^- in the reaction medium are accepted in equilibrium with unionized AzbT, experimental results can also be interpreted in another way: the amount of the more reactive Th_3 in the mixture affects and shifts the equilibrium between the two forms of AzbT. Hence, it seems that a higher AzbT:Th_3 molar ratio would shift the equilibrium towards AzbT polymerization into a linear chain, while a higher amount of Th_3 in the reaction medium displace this equilibrium toward AzbT-COO^- form. As previously assumed, this ionized form could work as a better dopant than BF_4^- for the PTh_3 growing chains that are developing faster due to the higher reactivity of Th_3.

For PTh_3, the C/S and B/F ratios, 4.6 and 0.23, respectively, are very close to those theoretically expected (*i.e.* 4.0 and 0.25, respectively). The detection of oxygen in this

homopolymer, with a C/O ratio of 17.5, was attributed to the oxidation of some Th rings, which also explains the small difference between the observed and theoretical C/S ratios. In the case of the 50:50 copolymer, the B/F ratio (0.19) and C/O ratio (5.0) are smaller than expected, while the N/B ratio (1.1) is not consistent with the incorporation of AzbT units into the copolymer chains. The same trends were founded from the calculated B/F, N/B and C/O ratios for the 60:40 copolymer (Table 1). These experimental data confirm the previous supposition about the multiple processes that can take place in the polymerization mixture of the above-mentioned copolymers. Generally when a film is forming from solution the moieties with the lower surface energy are naturally migrating toward the upper layers of it. In our particular case, the use of acetonitrile (polar and hydrophilic) as solvent could favours the migration toward these upper layers of the more hydrophilic and polar groups such as COOH groups. When considering 50:50 and 60:40 polymerization mediums, if AzbT works as dopant, rather than as comonomer, most of it will remain attached by electrostatic forces to the more hydrophobic PTh_3 chains in the deep layers of the film, fact that could explain the low values of N/B and C/O calculated ratios for these copolymers.

Finally, 80:20 P(AzbT-*co*-Th_3) presents a N/B ratio of 2.3, which reflects the incorporation of AzbT units into the copolymer chains. This feature is consistent with the C/N and C/O ratios (12.6 and 4.3, respectively), which indicates that the sources of N and O on the surface films are not only the BF_4^- dopant and the oxidation of Th rings, respectively, but also the incorporation of AzbT units.

Figure 3 depicts the characteristic XPS spectra in the C1s, O1s and N1s regions for PTh_3 and both 50:50 and 80:20 P(AzbT-*co*-Th_3). Deconvolution of the C1s peak led to

two or three Gaussian curves, depending on the sample. The component at ~284.5 eV, which is present in all samples, corresponds to the C–C/C=C (284.8 eV) linkages of the Th_3 and AzbT units.[68-70] The spectra recorded for PTh_3 and 50:50 P(AzbT-*co*-Th_3) (also for the 60:40 copolymer, Figure S6) show a component centered at ~286.4 eV, which has been attributed to the C–S bond of polarized Th rings.[68-71] This component is apparently absent in the 80:20 copolymer. Furthermore, the latter is the only composition that presents the component associated to the aromatic C=C–N groups from the AzbT units at 285.6 eV.[72] These features are fully consistent with the assumptions derived from the atomic compositions, according to which the amount of AzbT units in the 50:50 and 60:40 copolymers is very low, while AzbT is the main constituent of the 80:20 copolymer. The assignment of the components detected at 283.9 and 281.6 eV for PTh_3 and 50:50 P(AzbT-*co*-Th_3), respectively, is not so clear, even though they probably belong to the tetrabutylammonium cations and the substrate. The values of N/B ratios corroborated with the uniqueness of C–S bond of polarized Th rings in 50:50 and 60:40 copolymers and that of aromatic C=C–N groups in 80:20 copolymer sustain the supposition that AzbT could works not only as a comonomer but as the dopant, as well.

Deconvolution of the O1s peak obtained from PTh_3 (Figure 3) led to three Gaussian curves that have been attributed to the C=O arising from the oxidation of the Th rings (531.0 eV) and the inorganic oxides of the ITO electrode (528.9 and 527.2 eV).[73-75] For the 50:50 copolymer, the component of highest energy changes to 532.1 eV and has been associated to the O=C–O bonding,[45,76,77] while the other two components correspond to the oxides of ITO electrodes. The spectrum of the 80:20 copolymer shows two components centered at 532.4 and 531.3 eV that correspond to O=C–O and C=O bonds,

respectively. The high resolution XPS spectrum of the S2p region for PTh_3 and all P(AzbT-*co*-Th_3) compositions (Figure S7) is very similar to that recently reported for different PTh derivatives.[45,69,78] The main observations refer to the spin-split sulphur coupling, $S2p_{3/2}$ (163.6-163.9 eV) and $S2p_{1/2}$ (164.8- 165.1eV), with a separation of 1.2 eV, and to the relatively high energy broad tail produced by positively charged sulphur within the Th rings.

Finally, the high resolution N1s spectrum of PTh_3 in Figure 3 shows a single peak centred at 402.2 eV, which has been attributed to the $C–N^+$ bond of tetrabutylammonium counterions.[79] The N1s spectra recorded for the three P(AzbT-*co*-Th_3) compositions present two peaks centred at 402.1-402.6 and 399.3-399.8 eV. The former corresponds to the tetrabutylammonium counterion,[79] as it was identified for PTh_3, while the latter has been assigned to the C–N bond of AzbT units.[80] Although the amount of AzbT units is relatively low in the 50:50 and 60:40 copolymers (atomic percent composition of N associated to AzbT units: 0.1% and 0.4%, respectively), it is significantly higher for the 80:20 copolymer (2.8%).

The overall of the XPS analyses reveals some difficulties in determining the composition of the copolymer chains obtained using 50:50, 60:40 and 80:20 AzbT:Th_3 ratios in the generation medium. However, the morphologies and topographies of the three prepared copolymers are not only completely different when compared among them, but also with regard to those of PTh_3 (see next sub-section), which is consistent with different chemical compositions. On the basis of these results, we have concluded that the content of AzbT units in P(AzbT-*co*-Th_3) increases with the concentration of the

corresponding monomer in the generation medium, as it is clearly evidenced by the N1s XPS spectra.

FTIR Spectroscopy

Another attempt for assessing the composition of the synthesized copolymers was done by using FTIR spectroscopy. Unlike XPS spectroscopy, which is a surface sensitive quantitative technique not deeper than 5-10 nm, FTIR measurement is a "through the sample" technique. The experimental details concerning the recording are given in ESI, while the IR spectra of the polymer films are shown in Figure 4. By analysing of all the spectra in this figure it can be notice that they are approximately similar in their shape in the range 400 – 1280 cm^{-1}. The most evident peaks in this range appeared as follows: the peak at around 568 cm^{-1} attributable to γ thiophene ring vibration[60]; that at 695 cm^{-1} ± 4 cm^{-1} due to C–S–C ring deformation; and the peak at 793 cm^{-1} due to CH out-of-plane bending vibration (δ C–H) of 2,5-substituted thiophene rings.[81,82] A strong doublet-like band centered at 1260 cm^{-1} and at 1050 ± 10 cm^{-1} is also present in this range which could be due to the β C–H bending in doped PTh chains[81]. An absorption band centered at 1660 cm^{-1}± 20 cm^{-1} can be seen in the spectra of all the investigated materials due to the conjugation between the thiophene rings along the polymer chains.

Unlike PTh_3, P(AzbT-*co*-Th_3)s present in the range 1650-1800 cm^{-1} a discernible peak centered at approximately 1730 cm^{-1} that was attributed to the vibration of carbonyl (ν C=O) in carboxyl groups and that it is shifted by 40 cm^{-1} toward higher wave numbers by comparing with that in AzbT monomer, in a similar manner as observed before.[83] It should be noted that between this position and 1800 cm^{-1}, in all the spectra, there are

several peaks that could be due to the presence of other carbonyl moieties as it was already revealed by XPS analysis. There are several plausible explanations that would motivate the presence of these peaks in the spectra: *(i)* Despite all the precautions taken during the experiments, traces of moisture could be present in AzbT structural units due to its inherent molecular association with the carboxyl groups.[84] Thus, several works have shown that the presence of water traces results in the incorporation of carbonyl groups in the polymer chains when they are obtained by electropolymerization;[63] *(ii)* During the handling of the sample, a photo-oxidation process could occur. There are several possible mechanisms that could lead to the formation of carbonyl groups within a PTh backbone due to photo-oxidation,[85] but formation of carboxylic acids was ruled out by Holdcroft,[86] and recently it was reiterated for unsubstituted PTh.[87]

Based on the IR spectra presented in Figure 4, the copolymers composition was calculated by using the ratio of the integrated area of the peak at 1730 cm^{-1} (belonging only to the AzbT comonomer) and the integrated area of the peak at 793 cm^{-1} (belonging to both comonomers). The obtained results are presented in Table 1. The use for this calculation of one from the characteristic absorptions of 1,3,5-trisubstituted benzene ring was hindered by the overlapping of its characteristic bands with those of the thiophene ring.

From the results showed in Table 1, it can be concluded that the results of XPS analysis correlate well with those from IR investigation, reflecting that the highest amount of the AzbT comonomer is present in 80:20 copolymer. Furthermore, the AzbT:Th_3 ratio values obtained from IR spectra are almost the same for the 60:40 and 80:20 copolymers. Unfortunately, from IR analysis, it was not possible to further

discriminate between enchained AzbT units and AzbT-COO^- present in copolymers as dopant, due to the fact that the asymmetrical and symmetrical carbonyl stretching vibration in the ionized COO^- at approximately 1550 and 1425 cm^{-1},[84] respectively, merged with those of asymmetric and symmetric stretching vibrations of the thiophene ring. However, taking into account the XPS results and also the difference in shape of IR spectra it could be claimed that the highest amount of the enchained AzbT units are found in 80:20 copolymer.

Thickness, morphology and topography

Micrometric PTh_3 films were obtained using a polymerization time of 150 s (Table 2). The incorporation of AzbT monomer into the generation medium resulted in a drastic reduction in the thickness of the electropolymerized films. Thus, the thickness of all P(AzbT-*co*-Th_3) copolymers determined by profilometry was around ~400 nm (Table 2). In addition to that, scratched regions were further scanned by AFM. Although the thicknesses determined by analyzing the recorded AFM images (Figure 5) were in good agreement with the profilometry estimations, the values determined using the former technique were ~100-200 nm lower (Table 2). These results are fully consistent with our previously discussed interpretations according to which the presence of AzbT obstructs the polymerization of Th_3 units and favors the formation of compact cross-linked structures.

Figure 6 shows low, medium and high magnification SEM micrographs of all prepared materials, while AFM images are provided in Figure 7. PTh_3 presents a porous structure made of sub-micrometric sheets that aggregate at different levels. The topography

derived from such multileveled surface consists on a dense distribution of abundant peaks emerging from deep and narrow valleys. This particular distribution results in a relatively rough surface with a root mean square roughness (RMS Rq) value of 380±67 nm. The presence of AzbT in the polymerization medium drastically affects the structure, as it is evidenced in Figures 6 and 7. Thus, the surface morphology and topography of P(AzbT-*co*-Th_3) copolymers vary progressively with the content of AzbT in the polymerization medium. More specifically, the porous multi-leveled morphology of 50:50 P(AzbT-*co*-Th_3) largely reminds that of PTh_3, even though the surface of the former is significantly more flat than the one of the latter. The sheets become smaller and show folds in 60:40 P(AzbT-*co*-Th_3), resulting into a more compact morphology and smooth topography. Finally, the 80:20 copolymer presents a dense globular morphology, in which the sheets completely disappear, and are organized in a plane surface. The progressive reduction in the RMS roughness with the increasing content of AzbT in the polymerization medium is displayed in Table 2. Thus, the RMS Rq value decreases from 111±10 to 60±11 nm when the AzbT content increases in the polymerization medium.

Electrochemical and optical properties

Cyclic voltammetry studies were run to assess the influence of the presence of AzbT units on the electrochemical properties of P(AzbT-*co*-Th_3) films. Hence, the ability to exchange charge reversibly (*i.e.* electroactivity) and the electrochemical stability (*i.e.* electrostability) of the electropolymerized copolymers were evaluated by submitting the samples to ten consecutive oxidation-reduction cycles in acetonitrile (0.1 M TBATFB) from -0.4 to 1.1 V at different scan rates. Figure 8a represents the first control

voltammogram of PTh_3 and P(AzbT-*co*-Th_3) copolymers recorded at a scan rate of 100 mV/s. As it can be seen, the amount of exchanged charge (*i.e.* electroactivity) decreases with increasing the AzbT content in the polymerization medium. More specifically, the electroactivity of 50:50, 60:40 and 80:20 copolymers, which was determined by evaluating the oxidation and reduction charges from the corresponding voltammograms (Figure 8), is smaller than that of PTh_3 by 42%, 67% and 84%, respectively. Differences between PTh_3 and the three copolymers are independent of the scan rate, as it is evidenced in the control voltammograms recorded at 25 and 50 mV/s (Figure S8).

Although consecutive oxidation and reduction cycles provoked a reduction of electroactivity in all cases, the behavior of the copolymers differs from that of PTh_3 in terms of electrostability. Figure S9 compares the voltammogram recorded after 10 redox processes with that of the as prepared material (scan rate of 50 mV/s), while Figure 8b represents the variation of the electrostability (LEA in Eqn 1, ESI) with the scan rate for PTh_3 and P(AzbT-*co*-Th_3) samples.

The LEA value is lower than 7% for PTh_3, independently of the scan rate. The electrochemical stability decreases upon the incorporation of AzbT units, thus LEA values increase systematically with the content of AzbT in the polymerization medium. On the other hand, the low electrochemical stability of 80:20 P(AzbT-*co*-Th_3) is practically independent of the scan rate, whereas low scan rates affect negatively the electrochemical behaviour of the 50:50 and 60:40 copolymers.

Figure 9a represents the UV-vis spectra recorded for PTh_3 and P(AzbT-*co*-Th_3) films prepared using the experimental conditions described in the Methods section (ESI). For PTh_3, the broad absorption band centered at 475 nm, which corresponds to the π-π^*

transition, was used to approximate the optical π-π^* transition lowest transition energy (E_g = 1.64 eV) by estimating the onset wavelength (λ_{onset}= 758 nm). The spectrum of the 80:20 copolymer is very similar to that of PTh_3, and also displays a broad band centered at 447 nm (λ_{onset}= 677 nm). The resulting E_g value is 1.83 eV, which is slightly higher than that obtained for PTh_3.Accordingly, the extension of the π-conjugation is lower for 80:20 P(AzbT-*co*-Th_3) than for PTh_3. However, this reduction is more notable for the 50:50 and 60:40 copolymers, which show broad absorption bands at 392 and 400 nm, respectively. The E_g estimated for 50:50 and 60:40 P(AzbT-*co*-Th_3) are 1.94 (λ_{onset}= 634 nm) and 2.03 eV (λ_{onset}= 610 nm), respectively. It should be noted that these results are in excellent agreement with the doping level calculated from XPS interpretations.

Lastly, as polyazomethine-based materials have been reported to be used in electrochromic devices,[22,23] electrochromism was also examined for P(AzbT-*co*-Th_3) materials. The color of the as prepared films (Figure 9a) is dark blue for PTh_3, yellow-brownish for 50:50 and 60:40 copolymers, and earthy brown for 80:20 P(AzbT-*co*-Th_3). After being submitted to potentials of -0.40 (reduction process) and 1.40 V (oxidation process) during 100 s, PTh_3 and P(AzbT-*co*-films) exhibit a color change (Figure 10b). As it can be seen, the dark blue color of as prepared oxidized PTh_3 changes to bright orange upon reduction. The contrast is less marked for the three copolymers, which present brown and matt orange in the oxidized and reduced states, respectively. This feature suggests that the applicability of P(AzbT-*co*-Th_3) for the fabrication of electrochromic devices is limited if compared with PTh_3 and other PTh derivatives previously reported.[88-90]

Biological studies

Biocompatibility is a requisite when designing bioactive matrices for biotechnological and biomedical applications. Consequently, the interface in contact with cells is expected to guarantee no toxic or injurious effects on biological systems. To ensure that, biological studies were firstly performed by culturing MG-63 and Vero cells (human osteosarcoma and monkey kidney epithelial cell lines, respectively) in wells that contained ITO electrodes coated with PTh3 and P(AzbT-co-Th3) films. The 60:40 copolymer was not involved in such study since, as it was evidenced in previous subsections, its properties were very similar to those exhibited by 50:50 P(AzbT-co-Th3). By culturing cells in wells that contained uncoated ITO electrodes or only tissue culture polystyrene (TCPS) (*i.e.* no ITO electrode in the wells), controls were simultaneously performed.

By using the MTT assay the potential cytotoxicity of the systems was evaluated after 24 h and 7 days of culturing. All viable cells in the wells were quantified, which enabled us to consider the toxic effects associated not only to the polymeric matrix, but also to small molecules (*e.g.* acetonitrile, TBATFB, Th_3 and AzbT) or oligomers that could be eventually released from the polymeric matrix. Figure 10 indicates that PTh_3 and 50:50 copolymer reduce cells viability with respect to TCPS control after 24 h of culturing, thus exhibiting some cytotoxic effect for both MG-63 and Vero cell lines. In contrast, these negative effects are not observed for the 80:20 copolymer that shows viabilities slightly higher than those of the control. After 7 days, the cytotoxic effect of all studied systems on MG-63 cells disappears while PTh_3 and 50:50 P(AzbT-*co*-Th_3) samples remain toxic to Vero cells. The cytotoxicity of PTh_3 and 50:50 copolymer should be attributed to

harmful molecules, especially Th_3 monomers entrapped into the polymeric matrix, which are leaching out from the films. In a recent study, we found that Th_3 reaches a maximum of cytotoxicity when the concentration is ~10^{-5} M becoming stable at higher concentrations.[47] Although such observation is fully supported with the lack of negative effects for the copolymer obtained using the lowest concentration of Th_3 in the polymerization medium (Figure 10), the cytotoxicity of the AzbT monomer cannot be completely discarded yet and should be specifically analysed in future studies.

Figure 11 displays quantitative results for cell adhesion and proliferation assays. In this case cellular viability was exclusively determined onto the surface of uncoated (control) or coated ITO electrodes. General inspection of the results clearly evidence that Th_3 inhibits cell viability, which is fully consistent with the cytotoxic effect discussed above. The biocompatibility of the three examined organic materials clearly increases with the content of AzbT. Thus, the number of cells adhered to the surface of the 80:20 copolymer is considerably higher than that of PTh_3 and 50:50 P(AzbT-*co*-Th_3) films. Moreover, the adhesion and proliferation of MG-63 cells on the surface of 80:20 P(AzbT-*co*-Th_3) are also higher when compared to the results obtained for the control substrates (*i.e.* TCPS and uncoated ITO). In contrast, MG-63 cells activity on 50:50 P(AzbT-*co*-Th_3) is comparable to that observed for ITO, while PTh_3 shows the worst behavior as supportive matrix for cellular adhesion and proliferation. Regarding Vero cells, the biocompatibility of ITO, PTh_3 and 50:50 P(AzbT-*co*-Th_3) substrates is very poor, especially in terms of cell proliferation, whereas the cell response towards the 80:20 copolymer and control TCPS substrates is comparable.

Furthermore, the different ability exhibited byPTh_3 and the two examined P(AzbT-*co*-Th_3) copolymers to behave as cellular matrices is clearly reflected in the fluorescence microscopy images displayed in Figure S10. The densities of MG-63 and Vero cells adhered onto the substrate after 7 days of culturing, which are relatively low for PTh_3, increase considerably for the copolymers. In addition, the spreading of cells onto the surface of PTh_3 and 50:50 P(AzbT-*co*-Th_3) matrices is relatively inhomogeneous, becoming more uniform for the 80:20 copolymer. Details about the actin organization of cultured cells onto the investigated substrates are evidenced in the high magnification fluorescence images displayed in Figure 12. As it can be seen, cells tend to establish a large spreading of the cytoplasm in all cases, actin filaments being visible within the cells. Besides, cell-to-cell contact tends to be formed onto the copolymers surfaces, and thus the density of such connections increases with the content of AzbT units in the substrate. Hence, dense and large networks are obtained for both MG-63 and Vero cell lines adhered onto the 80:20 P(AzbT-*co*-Th_3) film.

SEM micrographs show MG-63 and Vero cells adhered and proliferated onto the surface of PTh_3 and P(AzbT-*co*-Th_3) films (Figure 13). Inspection of the images indicates that, in general, the receptivity of the polymeric surfaces to be colonized through cellular viability is higher for MG-63 cells than for Vero cells. Even though large microdomains without adhered Vero cells are identified on the surface of polymeric films (Figure 13b), proliferated Vero cells are widely spread. In contrast, the spreading of viable MG-63 cells indicates a homogeneous colonization for both adhered and proliferated cells (Figure 13a). These observations are fully consistent with the cell viability results and the fluorescence images recorded (Figures 11 and S10, respectively). On the other hand, high

magnification SEM micrographs provide details on the connection sites established between cells and the polymeric surfaces. These consist on long and thin actin filaments, which are known as filopodia, oriented towards the film surface for local adhesion. Filopodial protrusions play an important role in sensing, thus act as feelers of the substrate surface and participate in cell-cell interactions, which in turn control the adhesion of cells to the substrate and their migration through the surface (*i.e.* cellular motility).

Overall, the good results obtained for 80:20 P(AzbT-*co*-Th_3) films ensures its applicability as scaffolds in the field of tissue engineering.

CONCLUSIONS

A novel azomethine-containig bis-thienyl monomer, AzbT, has been synthesized by a simple chemical route. In spite of the easiness for its obtainment, the AzbT's structural peculiarities are responsible for both the impossibility of its electrochemical homopolymerization and the concomitant and complex phenomena that take place in the reaction medium when its copolymerization with Th_3 was applied.

XPS analyses as well as the FT-IR measurements of P(AzbT-*co*-Th_3) films evidenced that, near to copolymerization, other secondary processes are also developing in the reaction medium depending on AzbT:Th_3 molar ratios. The experimental results clearly corroborated that the content of AzbT in the copolymer chains increase with the content of AzbT in the electropolymerization medium and that, in the case of a higher amount of Th_3, AzbT works mostly as a dopant than as a comonomer. Differences in the structural, electrochemical and optical properties of the copolymers derived from the different

AzbT:Th_3 molar ratio support this feature. From a structural point of view, the thickness and roughness of P(AzbT-*co*-Th_3) films decrease with the content of AzbT. Furthermore, the porous multi-level surface morphology of the 50:50 copolymer, which is very similar to that of PTh_3, changes to a compact globular morphology in the 80:20 copolymer. On the other hand, the electroactivity and electrostability of the P(AzbT-*co*-Th_3) decreases with the content of AzbT, while the E_g depends on the molecular architecture of the copolymer chains, which is also affected by the AzbT content. Thus, the E_g of the 80:20 copolymer and PTh_3 are similar and lower than those of 50:50 and 60:40 P(AzbT-*co*-Th_3), which has been attributed to the cross-linked structure of the latters.

The potential application of P(AzbT-*co*-Th_3) films as bioactive substrates has been evaluated. Results obtained using human osteosarcoma and monkey kidney epithelial cell lines (MG-63 and Vero, respectively) indicated that the cytotoxicity of the examined systems increases with the content of Th_3, which has been attributed to the release of harmful Th_3 monomers entrapped into the polymeric matrix. The same tendency was observed for the cellular adhesion and proliferation assays. The 80:20 copolymer showed the best behavior as bioactive matrix. Indeed, cell viability has been found to be higher than for the control TCPS substrate. Furthermore, the spreading of cells cultured onto the surface of 80:20 P(AzbT-*co*-Th_3) is very homogeneous. In summary, film of this new copolymer promotes cellular viability, most probably due to the presence of the carboxyl groups. More specifically, we hypothesize that such favourable response is essentially due to the recognition of fibronectin and integrins from cells by the imine and carboxylate groups of AzbT units. It should be noted that, in a very recent study, such recognition mechanism was found to be responsible of the bioactive response of a

polythiophene:peptide composite.[48] Thus, the sequence of such short peptide, Cys-Arg-Glu-Lys-Ala (CREKA), was reported to contain a similar spatial distribution of the same functionalities.

On the other hand, if the antibacterial activity is *a priori* taken in account due to the presence of the Schiff base functionalities in its structure, thus it should be considered as a suitable bioactive platform for advanced biomedical applications in which optical properties similar to those displayed by semiconducting PThs derivatives are required.

ACKNOWLEDGEMENTS

Authors are in debt to support from MINECO and FEDER (MAT2012-34498). M.M.P.-M. thanks financial support through a FPI-UPC grant.

REFERENCES

1. K. Maruoka and T.Doi, *Chem.Rev.*, 2003, **103**, 3013.

2. T. Ooi and K. Maruoka, *Angew .Chem. Int. Ed.*, 2007, **46**, 4222

3. S. Li, S. Chen, S. Lei, H. Ma, R. Yu and D. Liu, *Corrosion Sci.*, 1999, **41**, 1273.

4. P. Mishra, H. Rajak and A. Mehta, *J. Gen. Appl. Microbiol.*, 2005, **51**, 133.

5. B.C. Revanasiddappa, M.A. jayamol and D. Satyanarayana, *Universal J. Pharm.*,2013, **2**, 145.

6. M. M. Ali, M. Jesmin, S. M. A. Salam, J. A. Khanam, M. F. Islam and M. N. Islam, *J. Sci. Res.*, 2009, **1**, 641.

7. M. de L. Ferreira, T. R. A. Vasconcelos, E. M. de Carvalho, M. C. S. Lourenço, S. M. S. V. Wardell, J. L. Wardell, V. F. Ferreira and M. V. N. de Souza, *Carbohydr. Res.*, 2009, **344**, 2042.

8. F. Martins, S. Santos, C. Ventura, R. Elvas-Leitão, L. Santos, S. Vitorino, M. Reis, V. Miranda, H. F. Correia, J. Aires-de-Sousa, V. Kovalishyn, D. A. R. S. Latino, J. Ramos and M. Viveiros, *Eur. J. Med. Chem*., 2014, **81**, 119.

9. Y. Zhou, M. Zhao, Y. Wu, C. Li, J. Wu, M. Zheng, L. Peng and S. Peng, *Bioorg. Med. Chem*., 2010, **18**, 2165.

10. M. S. Alam , J.-H. Choi and D.-U. Lee, *Bioorg. Med. Chem*., 2012, **20**, 4103.

11. K. V. Sashidhara, A. Kumar, G. Bhatia, M.M. Khan, A.K. Khanna and J.K. Saxena, *Eur.J. Med.Chem*., 2009, **44**,1813.

12. S. Ganguli, M. Firdous, T. S. Maity, R.K. Bera and M. Panigrahi, *Int. J. Pharm. Pharm. Sci*., 2012, **4**, 175..

13. K. S. Kumar, S. Ganguly, R. Veerasamy and E. De Clercq, *Eur.J. Med.Chem*., 2010, **45**, 5474.

14. K. M. Khan, M. Khan, M. Ali, M. Taha, S. Rasheed , S. Perveen and M. Iqbal Choudhary, *Bioorg. Med. Chem*., 2009, **17**, 7795.

15. M. Jesmin, M.M. Ali and J.A. Khanam, *Thai J. Pharm. Sci*., 2010, **34,** 20.

16. A. Iwan and D. Sek, *Prog. Polym Sci*., 2008, **33**, 289.

17. S. Barik and W.G. Skene, *Polym. Chem*., 2011, **2**, 1091.

18. S. Barik, T. Bletzacker and W.G. Skene, *Macromolecules*, 2012, **45**, 1165

19. A. Iwan, E. Schab-Balcerzak, K. P. Korona, S. Grankowska and M. Kaminska, *Synth. Met.*, 2013, **185– 186**, 17.

20. C. Mallet, M. Le Borgne, M. Starck and W. G. Skene, *Polym. Chem*., 2013, **4**, 250.

21. I. Kaya and M. Kamaci, *J. Fluoresc*., 2013, **23**, 115.

22. S. Tarkuc, E. Sahin, L. Toppare, D. Colak, I. Cianga and Y. Yagci, *Polymer*, 2006, **47**, 2001.

23. A. Bolduc and W. G. Skene, *Polym. Chem*, 2014, **5**, 1119.

24. D. Isık, C. Santato, S. Barik and W.G. Skene, *Org. Electron.*, 2012, **13**, 3022.

25. B. Hu, X. Zhu, X. Chen, L. Pan, S. Peng, Y. Wu, J. Shang, G. Liu, Q. Yan and R.-W. Li, *J. Am. Chem. Soc*., 2012, **134**, 17408..

26. J.-M. Lehn, *Prog. Polym Sci*, 2005, **30**, 814.

27. T. Maeda, H. Otsuka and A. Takahara, *Prog. Polym Sci*., 2009, **34**, 581.

28. E. Moulin, G. Cormos and N. Giuseppone, *Chem. Soc. Rev*., 2012, **41**, 1031.

29. N. Giuseppone, G. Fuks and J.-M. Lehn, *Chem. Eur. J*., 2006, **12**, 1723.

30. D. Janeliunas, P. van Rijn, J. Boekhoven, C.B. Minkenberg, J. van Esch and R. Eelkema, *Angew. Chem. Int. Ed*., 2013, **52**, 1998.

31. C.I. Simionescu, I. Cianga, M. Ivanoiu, Al. Duca, I. Cocarla and M. Grigoras, *Eur.Polym. J*., 1999, **35**, 587.

32. C.I. Simionescu, I. Cianga, M. Ivanoiu, A. Airinei, M. Grigoras and I. Radu, *Eur. Polym. J*., 1999, **35**, 1895.

33. C.I. Simionescu, M. Grigoras, I. Ciang and N. Olaru, *Eur.Polym. J*.,1998, **34**, 891.

34. M. Grigoras, I. Cianga, A. Farcas, G. Nastase and M. Ivanoiu, *Rev. Roum. Chim*., 2000, **45**, 703.

35. D. Colak, I. Cianga and A.E. Muftuoglu, *J. Polym. Sci. Part A: Polym. Chem*,2006, **44**, 724.

36. I. Cianga and M. Ivanoiu, *Eur. Polym. J*., 2006, **42**, 1922.

37. E. Armelin, A. L. Gomes, M. M. Pérez-Madrigal, J. Puigalí, L. Franco, L. J. del Valle, A. Rodríguez-Galán, J. S. de C. Campos, N. Ferre-Anglada and C. Alemán, *J. Mat. Chem.*, 2012, **22**, 585.

38. M. M. Pérez-Madrigal, E. Armelin, L. J. del Valle, F. Estrany and C. Alemán, *Polym. Chem.*, 2012, **3**, 979.

39. M. M. Pérez-Madrigal, M. I. Giannotti, G. Oncins, L. Franco, E. Armelin, J. Puiggalí, F. Sanz, L. J. del Valle and C. Alemán, *Polym. Chem.*, 2013, **4**, 568.

40. M. M. Pérez-Madrigal, M. I. Giannotti, E. Armelin, F. Sanz and C. Alemán, *Polym. Chem.*, 2014, 5, 1248.

41. M. M. Pérez-Madrigal, M. I. Giannoti, L. J. del Valle, L. Franco, E. Armelin, J. Puiggalí, F. Sanz and C. Alemán, *ACS Appl. Mater. Interfaces*, 2014, **6**, 9719.

42. E. Llorens, E. Armelin, M. M. Pérez Madrigal, L. J. del Valle, C. Alemán and J. Puiggalí, *Polymers*, 2013, **5**, 1115.

43. E. Llorens, M. M. Pérez-Madrigal, E. Armelin, L. J. del Valle, J. Puiggalí and C. Alemán, *RSC Adv.*, 2014, **4**, 15245.

44. M. Planellas, M. M. Pérez-Madrigal, L. J. del Valle, S. Kobauri, R. Katsarava, C. Alemán and J. Puiggalí, *Polym. Chem.*, 2015, **6**, 925.

45. A. D. Bendrea, G. Fabregat, L. Cianga, F. Estrany, L. J. del Valle, I. Cianga and C. Alemán, *Polym. Chem.*, 2013, **4**, 2709.

46. A. D. Bendrea, G. Fabregat, J. Torras, S. Maione, L. Cianga, L. J. del Valle, I. Cianga and C. Alemán, *J. Mater. Chem. B*, 2013, **1**, 4135.

47. S. Maione, G. Fabregat, L. J. del Valle, A. D. Bendrea, L. Cianga, F. Estrany and C. Alemán, *J. Polym. Sci.: Part B: Polym. Phys.*, 2015, **53**, 239.

48. G. Fabregat, B. Teixeira-Dias, L. J. del Valle, E. Armelin, F. Estrany and C. Alemán, *ACS Appl. Mater. Interfaces*, 2014, **6**, 11940.

49. D. E. López-Pérez, D. Aradilla, L. J. Del Valle and C. Alemán, *J. Phys. Chem. C*, 2013, **117**, 6607.

50. J. Soto-Delgado, J. Torras, L. J. del Valle, F. Estrany and C. Alemán. *RSC Adv.* 2015, **5**, 9189.

51. M. M. Pérez-Madrigal, L. J. del Valle, E. Armelin, C. Michaux, G. Roussel, E. A. Perpète and Carlos Alemán, *ACS Appl. Mater. Interfaces*, 2015, **7**, 1632.

52. N. Sarı and P. Gürkan, *Z. Naturforsch*., 2004, **59b**, 692.

53. G. G. Mohamed, M.M. Omar and A. M.M. Hindy, *Spectrochimica Acta Part A*, 2005, **62**, 1140.

54. M. Tumer, E. Akgu, S. Toroglu, A. Kayraldiz and L. Donbak, *J. Coord. Chem*., 2008, **61**, 2935.

55. Z. Zhang, C. Bi, D. Buac, Y. Fan, X. Zhang, J. Zuo, P. Zhang, N. Zhang, L. Dong and Q. Ping Dou, *J. Inorg. Biochem*., 2013, **123**, 1.

56. C. I. Ezugwu, O. T. Ujam, P. O. Ukoha and N. N. Ukwueze, *Chem Sci Trans*., 2013, **2**, 1118.

57. M. Onciu, *J. Appl. Polym. Sci*., 2007, **103,** 2013.

58. E. Hamciuc, C. Hamciuc, V.E. Musteata, Y. Kalvachev and A.Wolinska-Grabczyk, *High Perform. Polym.*, 2014, **26**, 175.

59. Y. Ozaytekin, *Polym. Compos*., 2014, **35**, 372.

60. M. Avram and G. D. Mateescu, “Spectroscopia în infraroşu aplicaţii în chimia organică”, Editura Tehnică Bucureşti, 1966.

61. S. Destri, I. A. Khotina and W. Porzio, *Macromolecules*, 1998, **31**, 1079.

62. L. Marin, M.D. Damaceanu and D. Timpu, *Soft Matter*, 2009, **7**, 1.

63. R. Kiebooms, R. Menon, K. Lee, “Synthesis, Electrical and Optical Properties of Conjugated Polymers” in Handbook of Advanced Electronic and Photonic Materials and Devices, vol.8, Conducting Polymers, H.S. Nalwa Ed., Academic Press, 2001, p. 15.

64. G. Li, G. Koßmehl, H.- P. Welzel, G. Engelmann, W.- D. Hunnius, W. Plieth, H. Zhu, *Macromol. Chem. Phys*., 1998, **199**, 525.

65. J. Li, K. Aoki, *J. Electroanal. Chem.*, 1998, 458, 155.

66. D. N. Hendrickson, J. M. Hollander and W. L. Jolly, *Inorg. Chem.*, 1970, **9**, 612.

67. R. Benoit, Y. Durand, B. Narjoux, G. Quintana and Y. Georges, LaSurface X-ray Photoelectron Spectroscopy Database, http://www.lasurface.com/database/liaisonxps.php (accessed December 2014).

68. S. A. Spanninga, D. C. Martin and Z. Chen, *J. Phys. Chem. C*, 2010, **114**, 14992.

69. C. D. Grande, M. C. Tria, G. Jiang, R. Ponnapati and R. Advincula, *Macromolecules*, 2011, **44**, 966.

70. S. Ahmad, M. Deepa and S. Singh, *Langmuir*, 2007, **23**, 11430.

71. T. R. Dillingham, D. M. Cornelison and S. W. Townsend, *J. Vac. Sci. Technol., A*,1996, **14**, 1494.

72. J. S. Stevens, A. C. de Luca, M. Pelendritis, G. Terenghi, S. Downes and S. L. M. Schroeder, *Surf. Interface Anal.*, 2013, **45,** 1238.

73. S. Sharma, R. W. Johnson and T. A. Desai, *Appl. Surf. Sci.*, 2003, **206**, 218.

74. K. L. Purvis, G. Lu, J. Schwartz and S. L. Bernasek, *J. Am. Chem. Soc.*, 2000, **122**, 1808.

75. J. Chastain and C. Roger, Handbook of X-ray Photoelectron Spectroscopy, 1995.

76. E. Kiss, I. Bertoti and E. I. Vargha-Butler, *J. Colloid Interf. Sci.*, 2002, **245**, 91.

77. V. I. Nefedoc, D. Gati, B. F. Dzhurinskii, N. P. Sergushin and V. Ya, *Russ. J. Inorg. Chem.*, 1975, **20**, 2307.

78. D. Aradilla, D. Azambuja, F. Estrany, J. I. Iribarren, C. A. Ferreira and C. Alemán, *Polym. Chem.*, 2011, **2**, 2548.

79. A. S. Vanini, J. P. Audouard and P. Marcus, *Corr. Sci.*, 1994, **36**, 1825.

80. F. Beguin, I.Rashkov, N. Manolova, R. Benoit, R. Erre and S. Delpeux, *Eur. Polym. J.*, 1998, **34**, 905.

81. X.-G. Li, J. Li, Q.-K. Meng, M.-R. Huang, *J. Phys. Chem. B*, 2009, **113**, 9718. See also Electronic Supporting information.

82. Peng, L. Zhang, J. Spires, C. Soeller, J. Travas-Sejdic, *Polymer*, 2007, **48**, 3413.

83. O. Bertran, E. Armelin, F. Estrany, A. Gomes, J. Torras, C. Aleman, *J. Phys. Chem B*, 2010, **114**, 6281.

84. L. Cianga, *High Perform. Polym.*, 2005, **17**, 117.

85. T. K. Kunz and M.O. Wolf, *Polym. Chem.*, 2011, **2**, 640.

86. M. S. A. Abdou and S. Holdcroft, Macromolecules, 1993, **26**, 2954.

87. M. Manceau, A. Rivaton, J.-L. Gardette, S. Guillerez and N. Lemaitre, *Polym. Degrad. Stab.*, 2009, **94**, 898.

88. R. Berridge, S. P.Wright, P.J. Skabara, A. Dyer, T. Steckler, A. A. Argun, J. R. Reynolds, W.H. Ross and W. J. Clegg, *Mater. Chem.*, 2007, **17**, 225.

89. M. Krompiec, I. Gridzka, M. Filapek, L. Shorka, S. Krompiec, M. Lapkowski, M. Kania and W. Danikiewicz, *Electrochim. Acta*, 2011, **56**, 8108.

90. D. Aradilla, J. Casanovas, F. Estrany, J. I. Iribarren and C. Alemán, *Polym. Chem.*, 2012, **3**, 436.

Table 1. Atomic percent composition (B1s, C1s, N1s, O1s, F1s and S2p) of PTh_3 and P(AzbT-*co*-Th_3) copolymers based on XPS and copolymers composition obtained from FTIR spectroscopy.

	B1s	**C1s**	**N1s**	**O1s**	**F1s**	**S2p**	**AzbT:Th_3 (%)[a]**
PTh_3	3.8	66.7	3.7	3.8	16.6	5.4	-
50:50 P(AzbT-*co*-Th_3)	1.3	69.6	1.4	14.0	6.8	6.8	16/84
60:40 P(AzbT-*co*-Th_3)	1.2	73.3	1.6	3.2	6.6	14.3	59/41
80:20 P(AzbT-*co*-Th_3)	2.2	64.4	5.1	14.9	9.7	3.7	61/39

[a] Copolymer composition based on FTIR.

Table 2. Properties of PTh_3 and P(AzbT-*co*-Th_3) copolymers: Doping level (DL, in number of positive charges per Th ring), polymerization charge (Q_{pol}, in mC/cm^2), thickness determined by profilometry and AFM inspection of scratched regions (ℓ_{prof} and ℓ_{AFM}, in nm), respectively), root mean square roughness (RMS Rq, in nm) and π-π^* transition lowest transition energy (E_g, in eV).

System	DL	Q_{pol}	ℓ_{profil}	ℓ_{AFM}	RMS Rq	E_g
PTh_3	0.71	54.3±8.1	2.26±0.37 μm	-	380±67	1.64
50:50 P(AzbT-*co*-Th_3)	0.19	40.4±10.9	415±78 nm	254±16	111±10	1.83
60:40 P(AzbT-*co*-Th_3)	0.08	38.4±5.7	388±86 nm	291±23	78±8	1.94
80:20 P(AzbT-*co*-Th_3)	0.59	49.4±10.3	451±91 nm	253±53	60±11	2.03

CAPTIONS TO FIGURES

Figure 1. (a) ^{1}H-NMR spectrum of azomethine-containing bis-thienyl monomer. (b) ^{13}C-NMR spectrum of AzbT in DMSO-d_6: (∗●) sign at 151.5 ppm corresponds to carbon atom in the 3,5-diamino benzoic acid of =C-NH_2 type while (∗∗●) for the carbon atom of =C-CO type. It is also interesting to notice that in the region 155.5 ppm – 152 ppm for each conformer of the azomethine bond is present a peak for AzbT and the nonsymmetrical red compound. The breaking of the azomethine linkage is evidenced by the appearance of the 5-thiophene aldehyde in the mixture solution the characteristic peak of which is present at 184.21ppm. The appearance of three peaks in the range 165 ppm – 170 ppm proves that in the system are present three compounds containing carboxyl groups.

Figure 2. Control voltammograms for the oxidation of (a) Th_3, (b) 50:50 AzbT:Th_3, and (c) 80:20 AzbT:Th_3 in acetonitrile containing 0.1 M TBATFB. Voltammograms were recorded using 1.0×0.5 cm^2 ITO substrates as working electrodes. Initial and final potentials: 0.00 V; reversal potential: 2.10 V. Scan rate: 50 mV/s. The anodic processes (O) are indicated for each case.

Figure 3. High-resolution XPS spectra (black line) for PTh_3 and both 50:50 and 80:20 P(AzbT-*co*-Th_3): C1s (top), O1s (middle) and N1s (bottom) regions. Peaks from deconvolution (grey lines) are also displayed.

Figure 4. FTIR spectra of PTh_3 and 50:50, 60:40 and 80:20 P(AzbT-*co*-Th_3) copolymers.

Figure 5. AFM steps of (a) 50:50, (b) 60:40 and (c) 80:20 P(AzbT-*co*-Th_3) copolymers. Stars indicate the ITO surface.

Figure 6. SEM micrographs with different magnifications for PTh_3 and P(AzbT-*co*-Th_3): (a) PTh_3; (b) 50:50 P(AzbT-*co*-Th_3); (c) 60:40 P(AzbT-*co*-Th_3); and (d) 80:20 P(AzbT-*co*-Th_3).

Figure 7. 3D and 2D AFM height images for: (a) PTh_3; (b) 50:50 P(AzbT-*co*-Th_3); (c) 60:40 P(AzbT-*co*-Th_3); and (d) 80:20 P(AzbT-*co*-Th_3). Left column: 10 μm × 10 μm; right column 2 μm × 2 μm. (e) Cross-section profiles of a diagonal line for images (a) to (d).

Figure 8. (a) First control voltammogram for PTh_3 and P(AzbT-*co*-Th_3) in acetonitrile with 0.1M TBATFB. Initial and final potential: 0.0 V; reversal potential: 1.1 V. Scan rate: 100 mV/s. (b) Variation of the LEA (Eqn 1 in ESI) for PTh_3 and P(AzbT-*co*-Th_3) as a function of the scan rate.

Figure 9. (a) UV-vis spectra and color of as prepared PTh_3 and P(AzbT-*co*-Th_3) films. (b) Color of PTh_3 and P(AzbT-*co*-Th_3) films after applying a potential of 1.40 and -0.40 V during 100 s (oxidized and reduced samples, respectively).

Figure 10. Cytotoxicity of PTh_3 and P(AzbT-*co*-Th_3) films after 24 h and 7 days: (a) MG-63 and (b) Vero cells. Four samples were analyzed for each group. Bars represent the mean standard deviation. The relative viability of MG-63 and Vero cells was established in relation to the TCPS control (tissue culture polystyrene). ITO was also considered as a control substrate because PTh_3 and P(AzbT-*co*-Th_3) were deposited onto this material. The asterisk (*) indicates a significant difference with the TCPS control, Tukey's test ($p < 0.05$).

Figure 11. Relative cellular adhesion (viability onto the material after 24 h) and cellular proliferation (viability onto the material after 7 days) of PTh_3 and P(AzbT-*co*-

Th_3) films: (a) MG-63 and (b) Vero cells. Four samples were analyzed for each group. Bars represent the mean standard deviation. The relative viability of MG-63 and Vero cells was established in relation to the TCPS control (tissue culture polystyrene). ITO was also considered as a control substrate because PTh_3 and P(AzbT-*co*-Th_3) were deposited onto this material. The double asterisk (**) indicates a significant difference with the PTh_3 result, Tukey's test ($p < 0.05$).

Figure 12. High magnification fluorescence images of MG-63 and Vero cells (left and right, respectively) adhered onto: (a) ITO; (b) PTh_3; (c) 50:50 P(AzbT-*co*-Th_3); and (d) 80:20 P(AzbT-*co*-Th_3). Networks of cell-to-cell connections are displayed in (c) and (d) (dashed circles). Cell adhesion was observed with nuclei staining using Hoechst 33342.

Figure 13. SEM images for PTh_3 and P(AzbT-*co*-Th_3) covered with (a) MG-63 and (b) Vero cells: (#1) PTh_3; (#2) 50:50 P(AzbT-*co*-Th_3); and (#3) 80:20 P(AzbT-*co*-Th_3). From right to left columns: adhesion (1 kX), adhesion details, proliferation (1 kX) and proliferation details. Stars indicate the polymer surface.

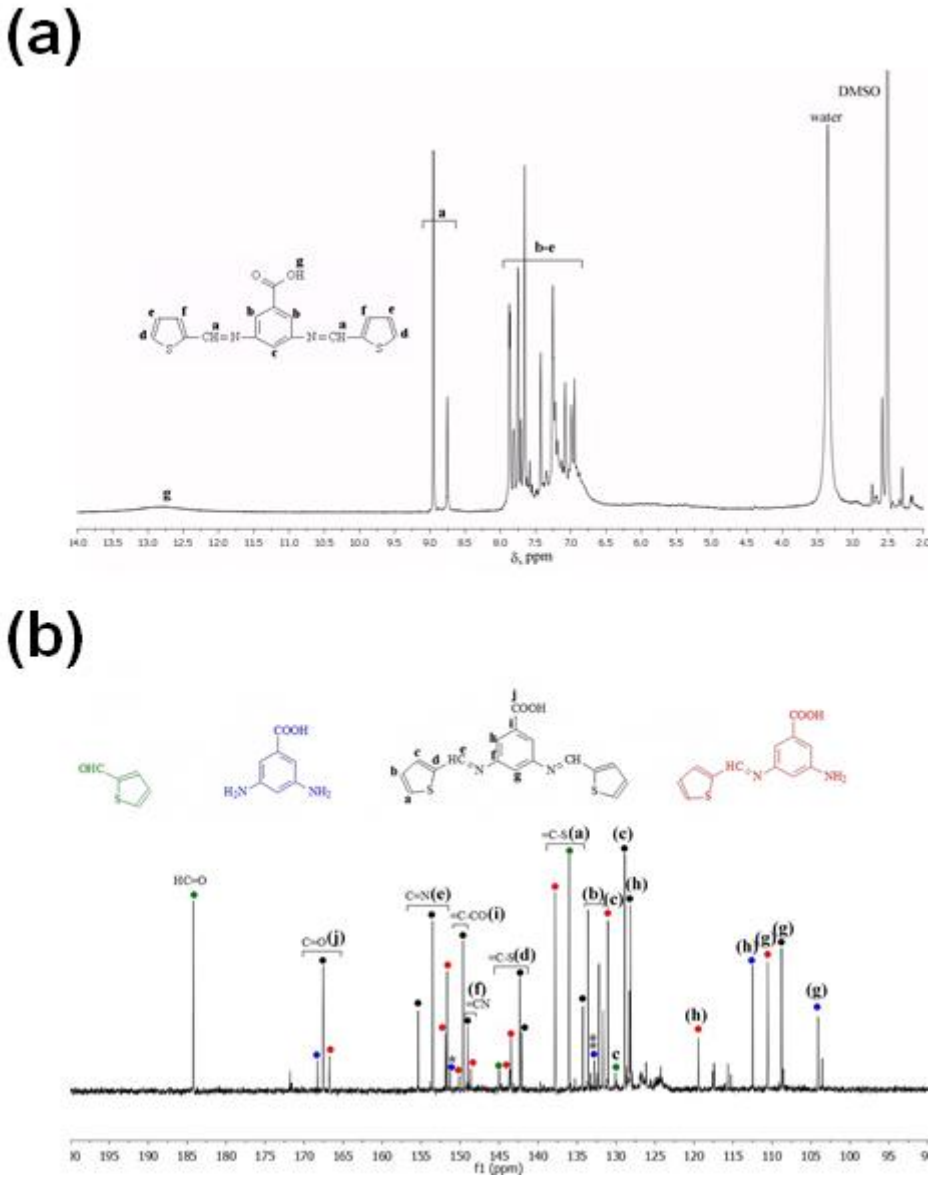
(a)
DMSO
water
a
b-e
g
δ, ppm
(b)
COOH
HC=O
C=O(j)
C=N(e)
=C-CO(i)
=C-S(d)
=C-S(a)
(c)
(b)
(h)
(f)
(g)
f1 (ppm)

Figure 1

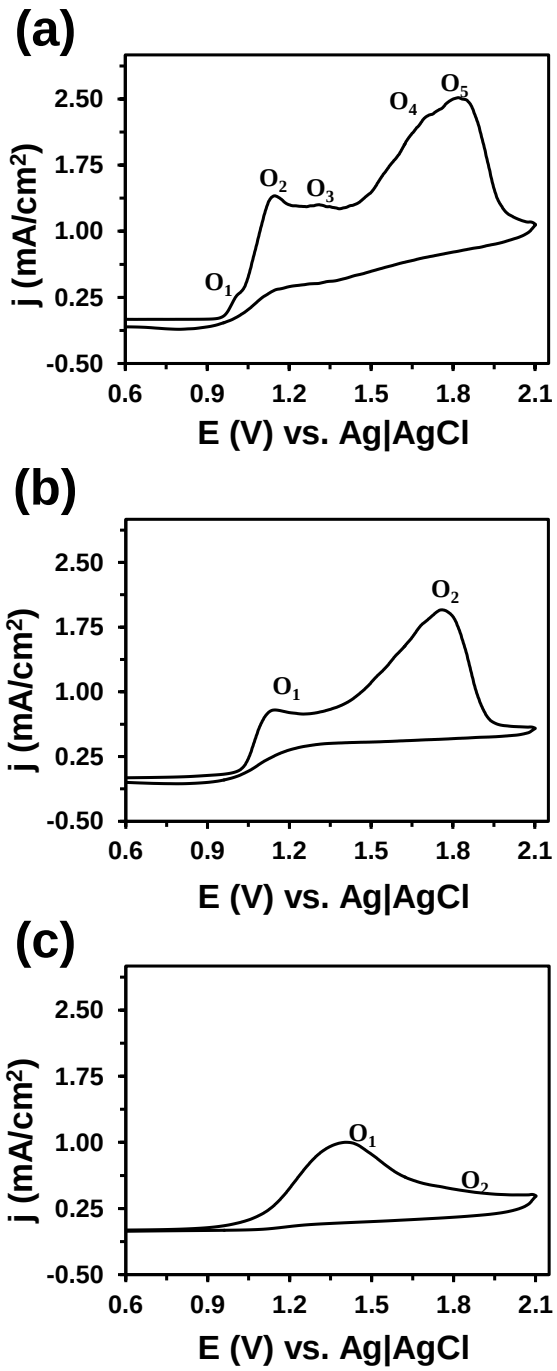
(a)
2.50
1.75
1.00
0.25
-0.50
j (mA/cm²)
O1
O2
O3
O4
O5
0.6
0.9
1.2
1.5
1.8
2.1
E (V) vs. Ag|AgCl
(b)
2.50
1.75
1.00
0.25
-0.50
j (mA/cm²)
O1
O2
0.6
0.9
1.2
1.5
1.8
2.1
E (V) vs. Ag|AgCl
(c)
2.50
1.75
1.00
0.25
-0.50
j (mA/cm²)
O1
O2
0.6
0.9
1.2
1.5
1.8
2.1
E (V) vs. Ag|AgCl

Figure 2

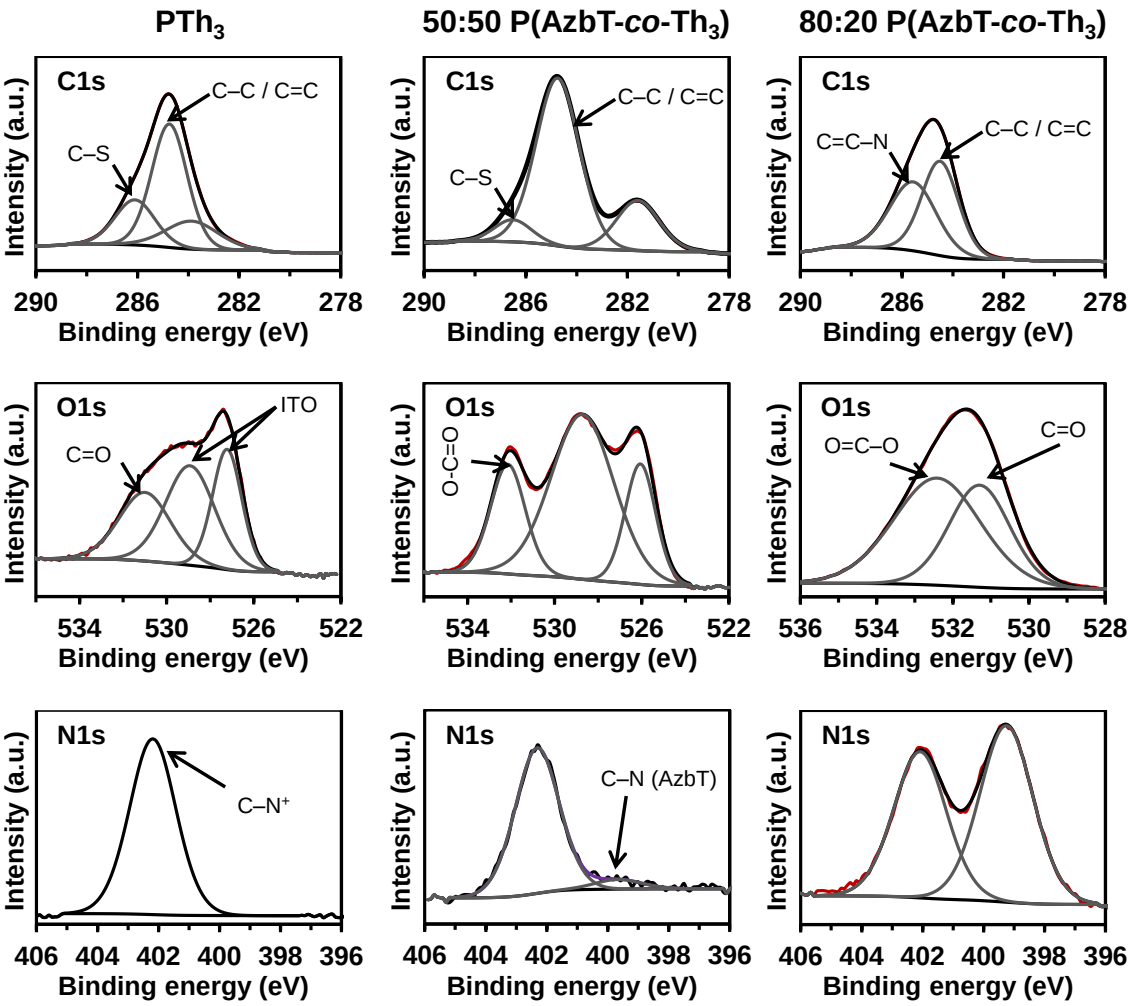
PTh3
50:50 P(AzbT-co-Th3)
80:20 P(AzbT-co-Th3)
C1s
C–C / C=C
C–S
C=C–N
O1s
C=O
ITO
O-C=O
O=C–O
N1s
C–N+
C–N (AzbT)
Intensity (a.u.)
Binding energy (eV)

Figure 3

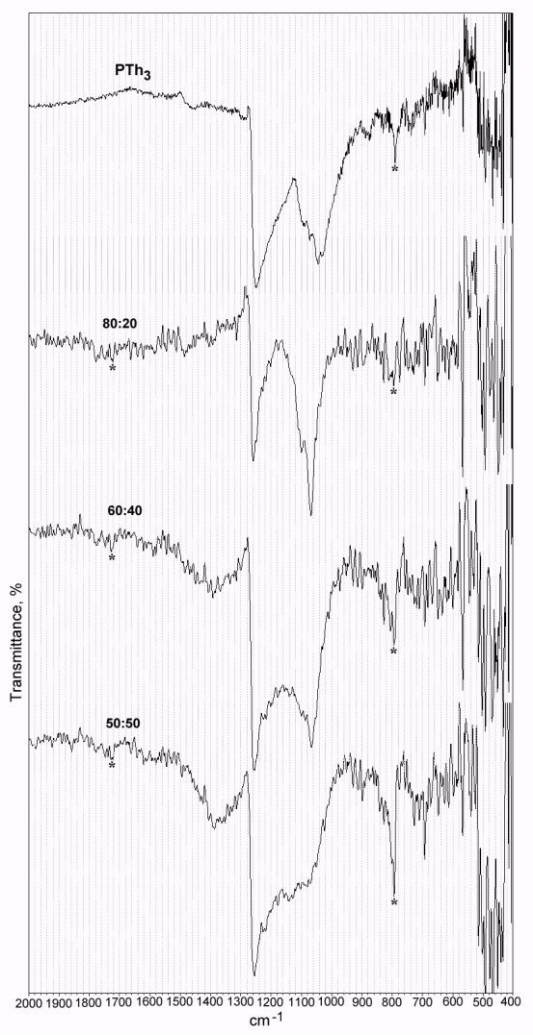
PTh3
80:20
60:40
50:50
Transmittance, %
2000 1900 1800 1700 1600 1500 1400 1300 1200 1100 1000 900 800 700 600 500 400
cm-1

Figure 4

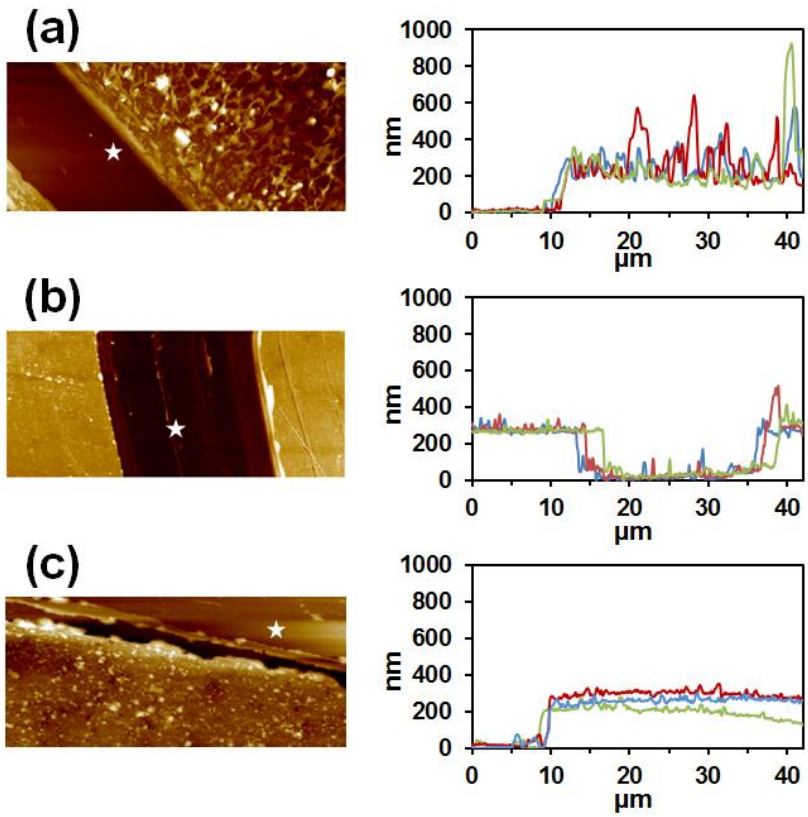

Figure 5

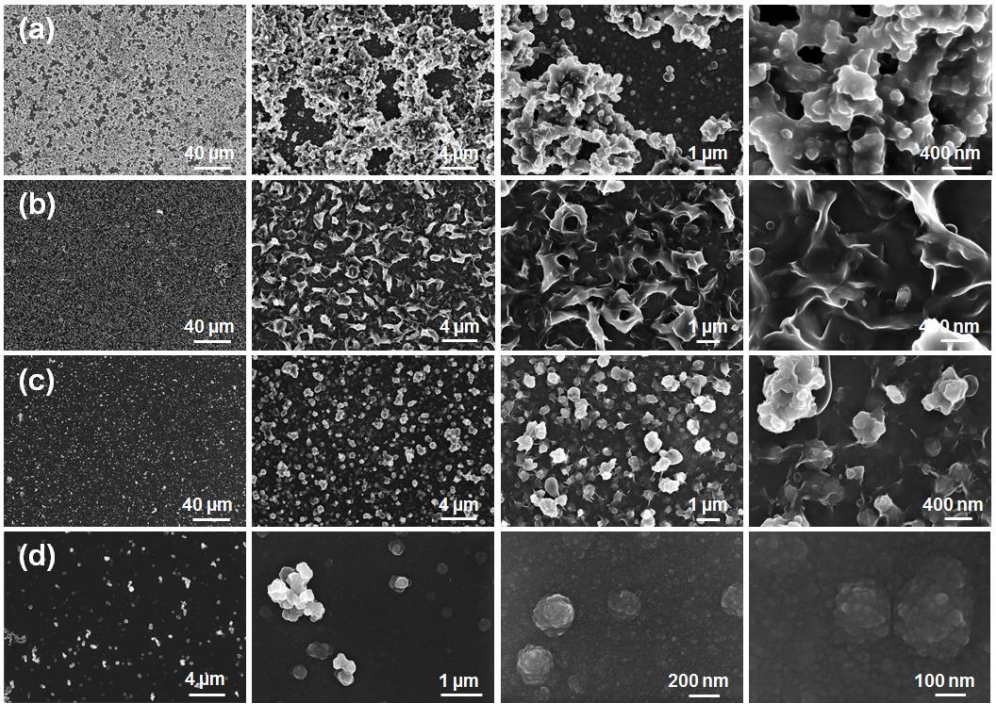
(a)
40 µm
4 µm
1 µm
400 nm
(b)
40 µm
4 µm
1 µm
(c)
40 µm
4 µm
1 µm
400 nm
(d)
4 µm
1 µm
200 nm
100 nm

Figure 6

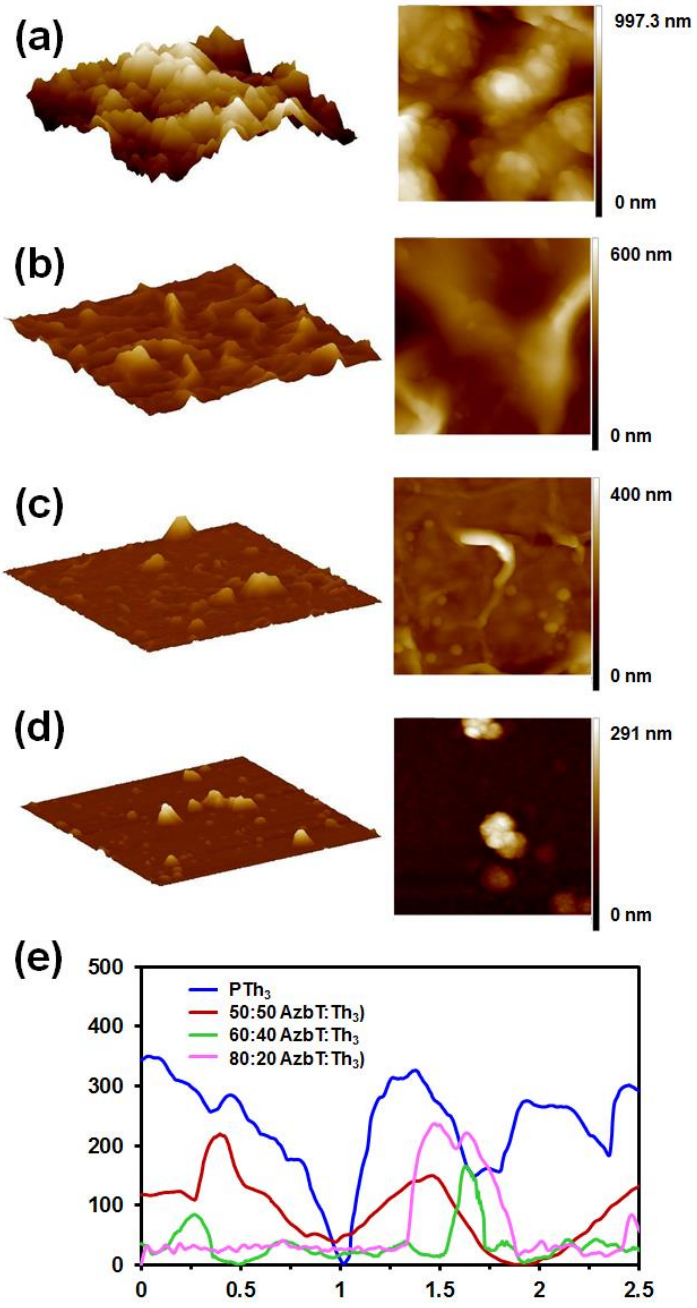
(a)
997.3 nm
0 nm
(b)
600 nm
0 nm
(c)
400 nm
0 nm
(d)
291 nm
0 nm
(e)
PTh3
50:50 AzbT:Th3)
60:40 AzbT:Th3
80:20 AzbT:Th3)
500
400
300
200
100
0
0
0.5
1
1.5
2
2.5

Figure 7

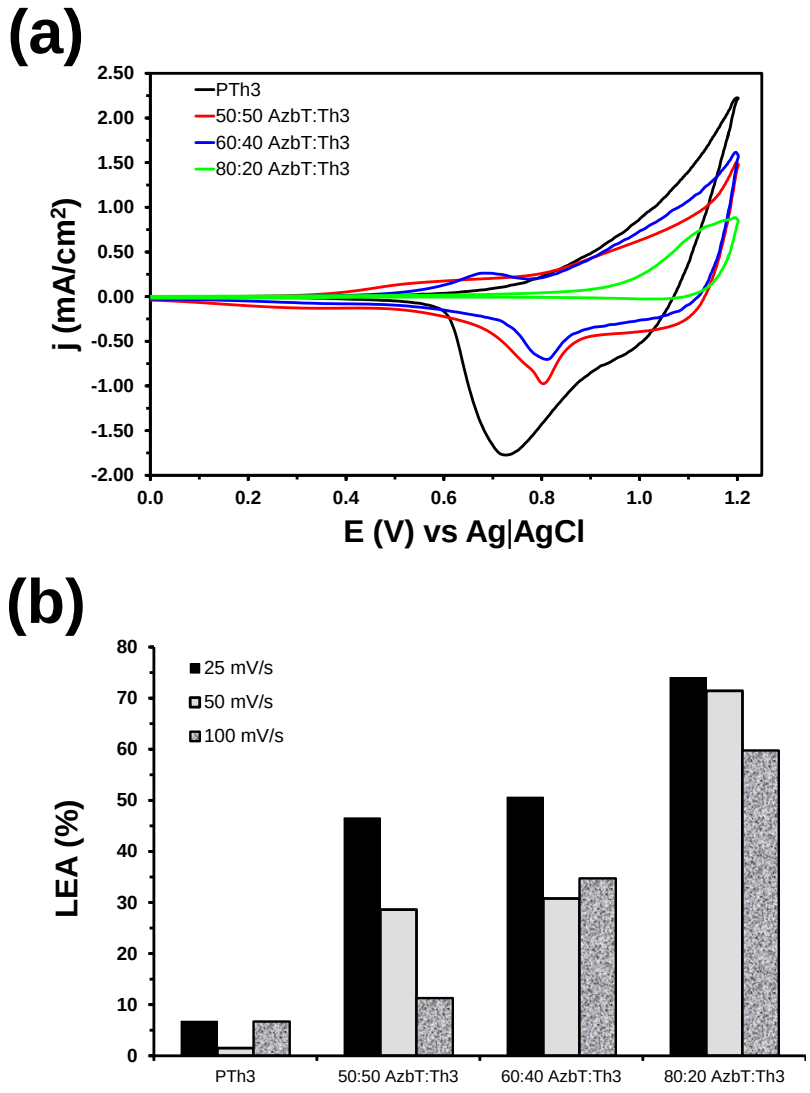
(a)
PTh3
50:50 AzbT:Th3
60:40 AzbT:Th3
80:20 AzbT:Th3
j (mA/cm²)
E (V) vs Ag|AgCl
(b)
25 mV/s
50 mV/s
100 mV/s
LEA (%)
PTh3
50:50 AzbT:Th3
60:40 AzbT:Th3
80:20 AzbT:Th3

Figure 8

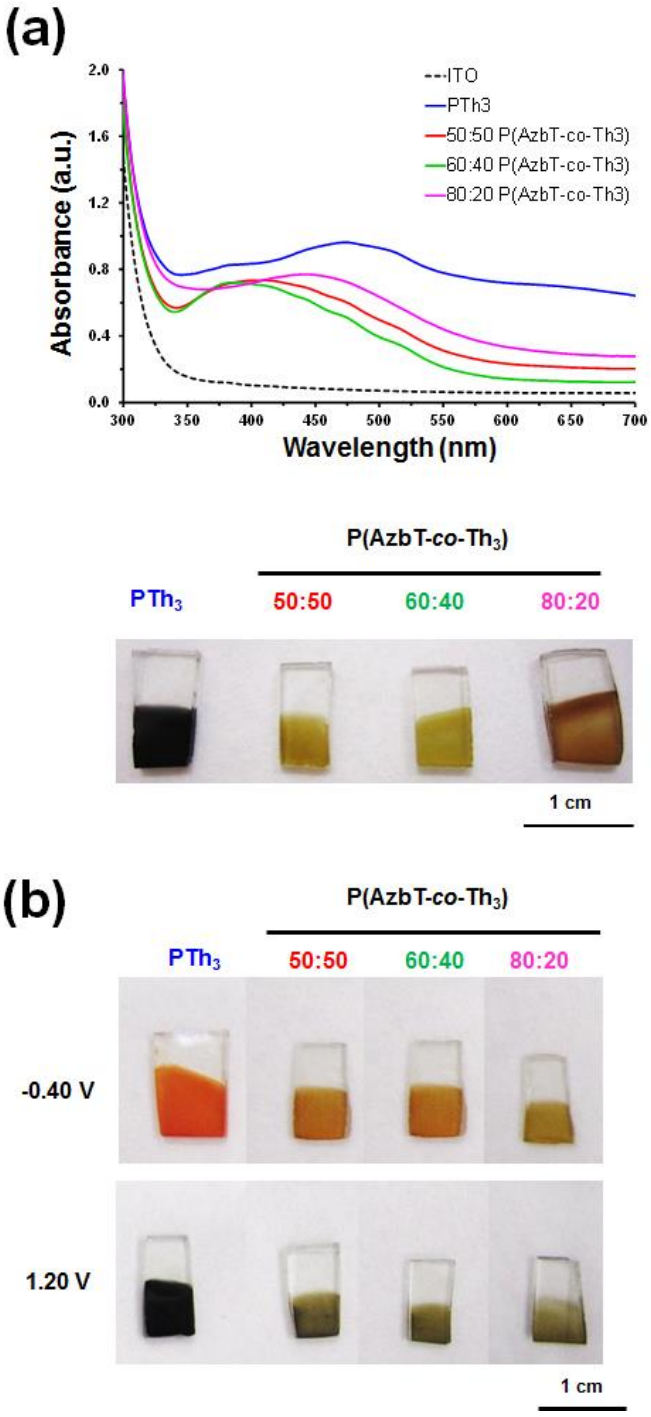
(a)
ITO
PTh3
50:50 P(AzbT-co-Th3)
60:40 P(AzbT-co-Th3)
80:20 P(AzbT-co-Th3)
Absorbance (a.u.)
Wavelength (nm)
P(AzbT-co-Th3)
PTh3
50:50
60:40
80:20
1 cm
(b)
P(AzbT-co-Th3)
PTh3
50:50
60:40
80:20
-0.40 V
1.20 V
1 cm

Figure 9

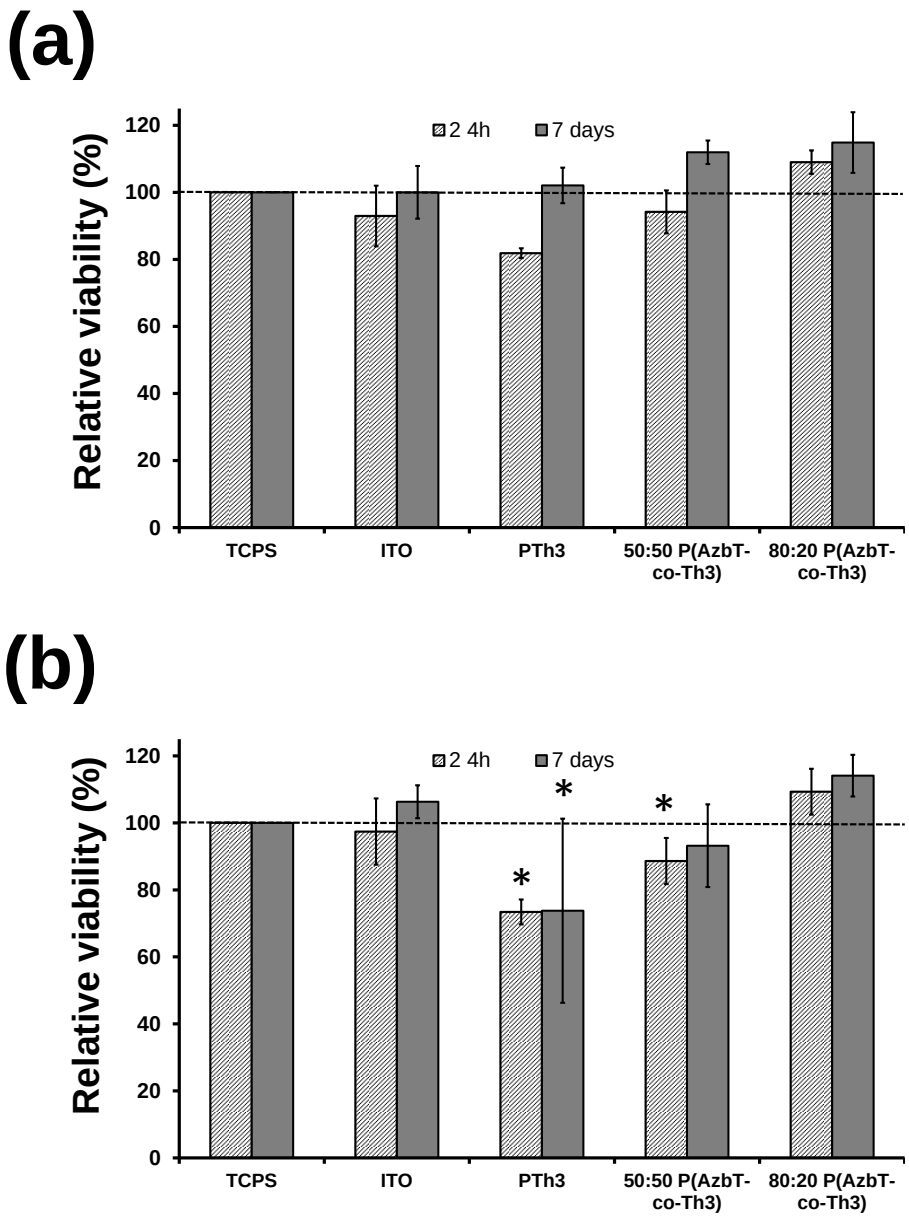
(a)
2 4h
7 days
Relative viability (%)
120
100
80
60
40
20
0
TCPS
ITO
PTh3
50:50 P(AzbT-co-Th3)
80:20 P(AzbT-co-Th3)
(b)
2 4h
7 days
Relative viability (%)
120
100
80
60
40
20
0
*
*
*
TCPS
ITO
PTh3
50:50 P(AzbT-co-Th3)
80:20 P(AzbT-co-Th3)

Figure 10

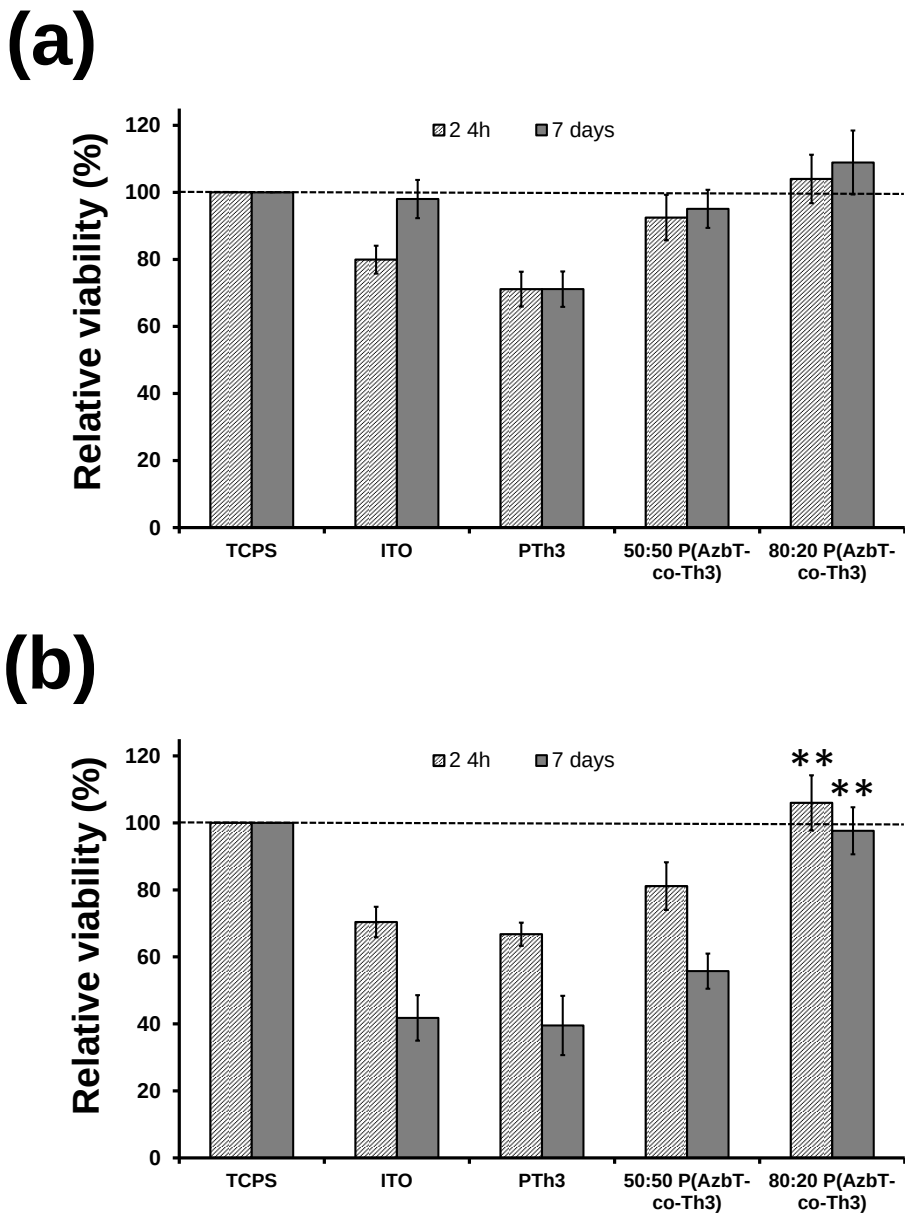
(a)
Relative viability (%)
120
100
80
60
40
20
0
2 4h
7 days
TCPS
ITO
PTh3
50:50 P(AzbT-co-Th3)
80:20 P(AzbT-co-Th3)
(b)
Relative viability (%)
120
100
80
60
40
20
0
2 4h
7 days
**
**
TCPS
ITO
PTh3
50:50 P(AzbT-co-Th3)
80:20 P(AzbT-co-Th3)

Figure 11

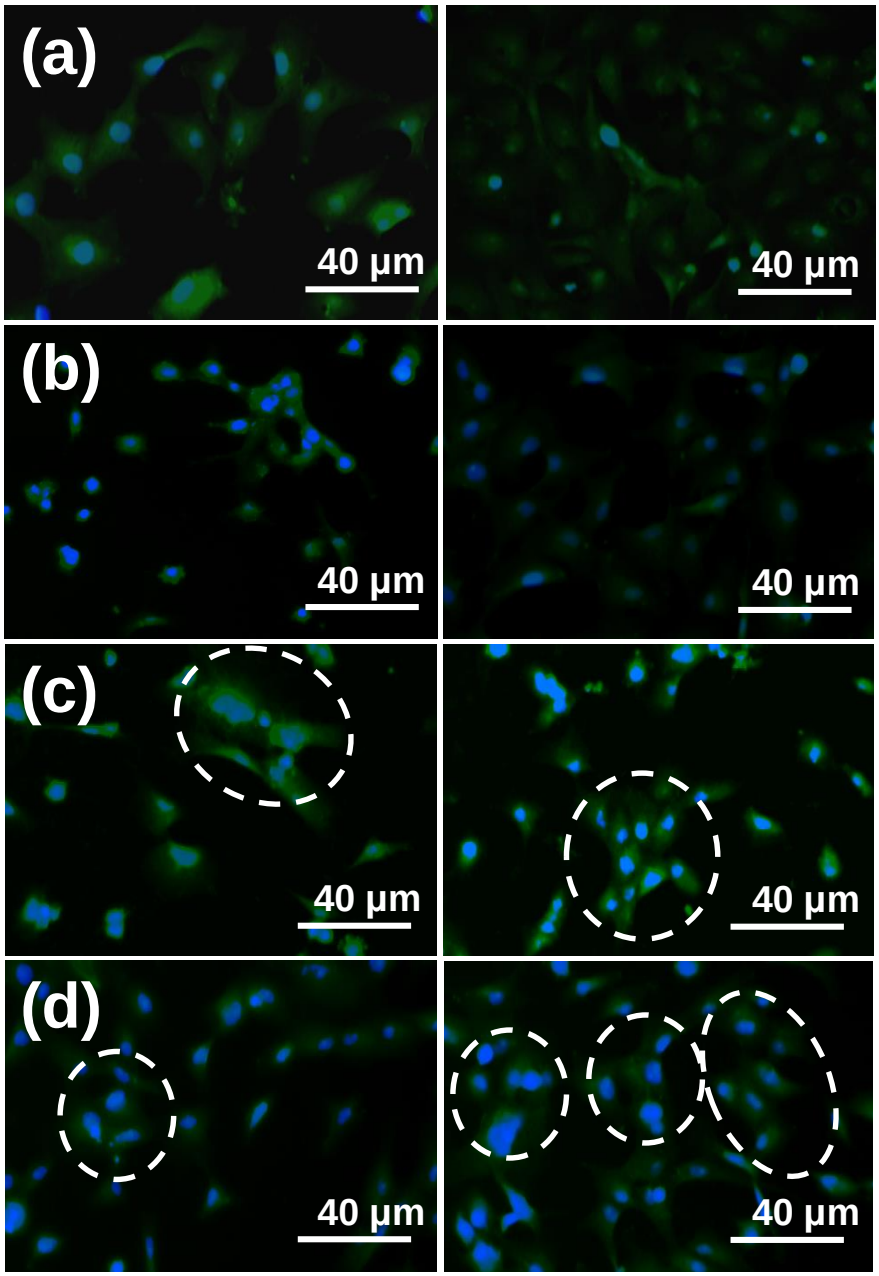

Figure 12

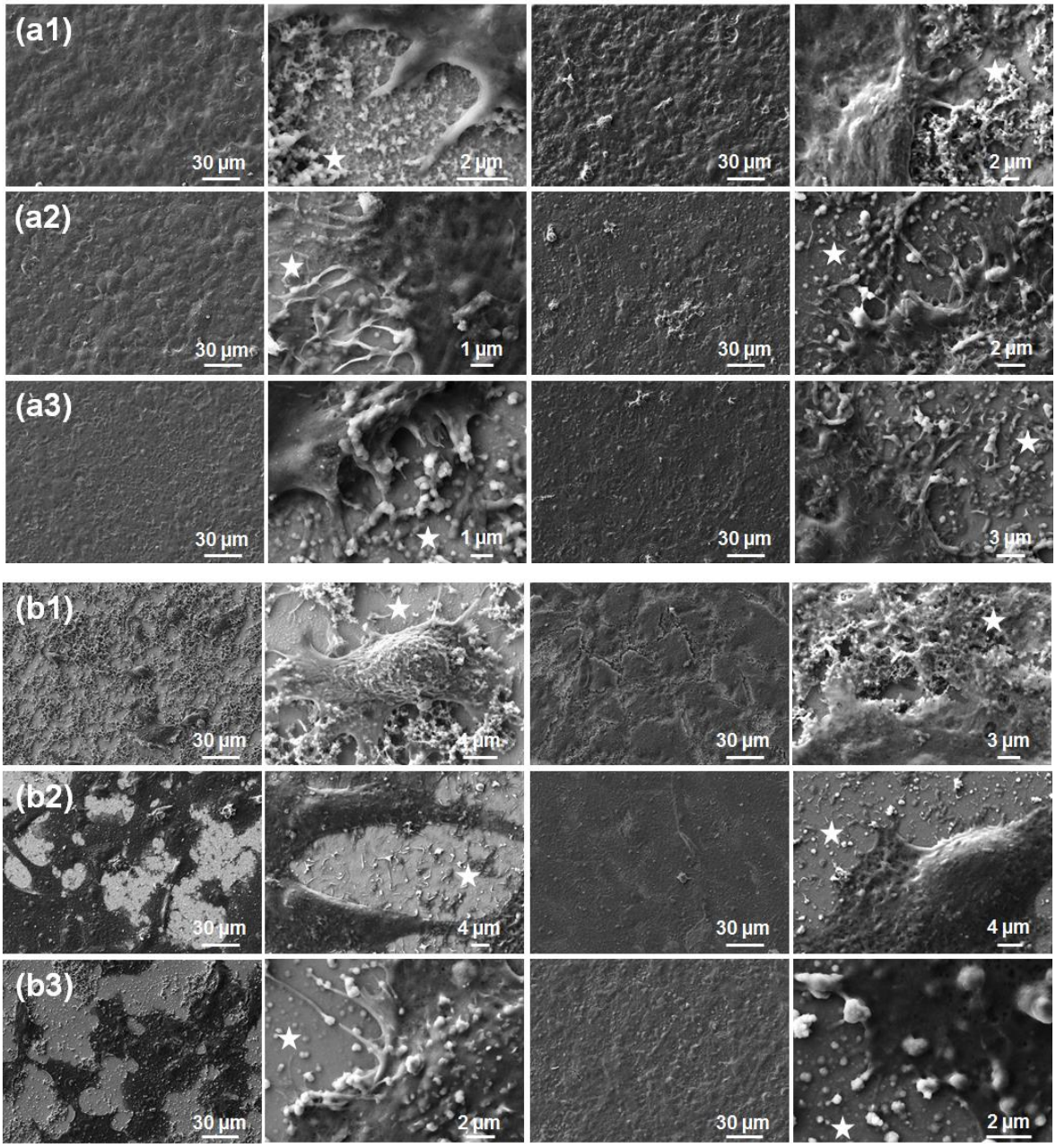
(a1)
30 μm
2 μm
30 μm
2 μm
(a2)
30 μm
1 μm
30 μm
2 μm
(a3)
30 μm
1 μm
30 μm
3 μm
(b1)
30 μm
4 μm
30 μm
3 μm
(b2)
30 μm
4 μm
30 μm
4 μm
(b3)
30 μm
2 μm
30 μm
2 μm

Figure 13

Graphical Abstract

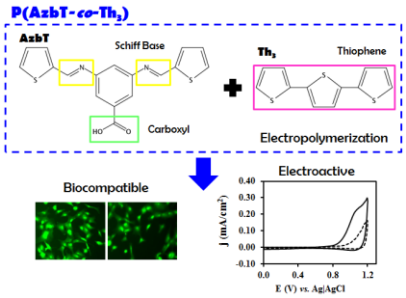

Copolymers made of a bis-thienyl monomer with preformed azomethine linkages and terthiophene are promising functional biomaterials